C. R. Palevol 14 (2015) 527–548

Contents lists available at ScienceDirect

Comptes Rendus Palevol

www.sciencedirect.com

General Palaeontology, Systematics and Evolution (Vertebrate Palaeontology)

Neck motion in turtles and its relation to the shape of the temporal skull region

Mouvement du cou chez les tortues et sa relation avec la forme de la zone temporale du crâne

Ingmar Werneburg [a,b]

[a] *Museum für Naturkunde, Leibniz-Institut für Evolutions-und Biodiversitätsforschung an der Humboldt-Universität zu Berlin, Invalidenstraße 43, 10115 Berlin, Germany*
[b] *Humboldt-Universität zu Berlin, Institut für Biologie, Philippstr. 13, 10115 Berlin, Germany*

ARTICLE INFO

Article history:
Received 22 August 2014
Accepted after revision 26 January 2015

Handled by Michel Laurin

Keywords:
Testudines
Proganochelys quenstedti
Neck retraction
Emargination
Fenestration
Principal component analysis

ABSTRACT

Extant turtles are characterized by diverse marginal reductions in their temporal skull region. Among other minor factors, their modes of neck retraction were hypothesized to have a key influence for shaping that region through evolution. A recent study on the mobility of the turtle neck highlighted the possibility that stem turtles, such as *Proganochelys quenstedti* were able to easily retract their necks by laterally tucking the skull under the anterior edge of the shell. A small emargination in the "cheek" of this species could be correlated to its mode of neck retraction. In the present study, by using a geometric morphometric approach, I correlated the curve shapes of retracted necks and other neck positions with the expansion of marginal reductions in turtle skulls. I hypothesize based on morphospace distributions that neck retraction evolved only once within turtle evolution and that pleurodiran and cryptodiran turtle retraction are directly and independently derived from ancestral neck tucking. Pleurodires evolved a middle kink in their elongated neck for lateral retraction. At the dawn of turtle evolution, associated to the ancestrally retracted (laterally rotated) neck, the cervicals were less specialized than in extant taxa. For cryptodires, that condition may have permitted a transitional, intervertebral rotation towards the vertical neck orientation found in that group during retraction. It retained the ancestral characteristically oriented curvature of the cervical column. I found that the cryptodiran mode of retraction and the ventral neck flexion in all turtles are strongly correlated to the expansion of the occiput emargination. Pleurodiran retraction, however, does not influence skull shape to such a degree. The "cheek" emargination is correlated with the expansion of the "occiput" emargination and appears to occur in correlation to the fixation of the palatoquadrate to the braincase in crown turtles. Neck related forces acting on the skull and ventral neck flexion are also hypothesized to be crucial factors for the reduction of a potential temporal fenestration inherited from a potentially fenestrated turtle ancestor.

E-mail address: i.werneburg@gmail.com

http://dx.doi.org/10.1016/j.crpv.2015.01.007
1631-0683/

Mots clés :
Testudines
Proganochelys quenstedti
Rétraction du cou
Émargination
Fenestration
Analyse en composantes principales

RÉSUMÉ

Les tortues actuelles sont caractérisées par diverses réductions marginales dans la zone temporelle de leur crâne. Parmi d'autres facteurs mineurs, il est supposé que leurs modes de rétraction du cou ont une influence capitale sur la forme de cette zone au cours de l'évolution. Une étude récente sur la mobilité du cou des tortues souligne la possibilité qu'a la souche de tortues, telles que *Proganochelys quenstedti* d'être capable de rétracter aisément le cou en le rentrant sous le bord antérieur de la carapace. Une petite émargination dans la « joue » de cette espèce pourrait être corrélée avec son mode de rétraction du cou. Dans la présente étude, en utilisant une approche morphométrique géométrique, l'auteur corrèle les formes de courbure des cous rétractés et d'autres positions du cou, avec l'extension des réductions marginales dans le crâne des tortues. Et il fait l'hypothèse, fondée sur les répartitions de « morphospaces », que la rétraction du cou évolue une fois au cours de l'évolution de la tortue et que la rétraction du cou chez les tortues pleurodires et cryptodires est directement et indépendamment dérivée de la pliure de cou ancestrale. Les Pleurodires développent une boucle médiane dans leur cou allongé, pour une rétraction latérale. À l'aube de l'évolution, associées au cou rétracté (tourné latéralement) ancestral, les cervicales sont moins spécialisées que chez les taxons actuels. Pour les cryptodires, cette condition peut avoir permis une rotation intervertébrale transitionnelle vers l'orientation verticale du cou, trouvée dans ce groupe au cours de la rétraction. Ceci maintient la courbure ancestrale orientée de manière caractéristique de la colonne cervicale. L'auteur trouve que le mode de rétraction de type cryptodire et la flexion ventrale du cou chez toutes les tortues sont fortement corrélés avec l'extension de l'émargination de l'occiput. Néanmoins, la rétraction de type pleurodire n'influence pas autant la forme du crâne. L'émargination de la « joue » est corrélée avec l'extension de l'émargination de « l'occiput » et paraît en corrélation avec la fixation du palato-carré à la boîte crânienne chez les tortues couronnées. Une hypothèse peut aussi être formulée, selon laquelle les forces liées au cou agissant sur le crâne et la flexion ventrale du cou peuvent être des facteurs cruciaux pour la réduction d'une fenestration temporale potentielle, héritée d'un ancêtre tortue potentiellement fenestré.

1. Introduction

Traditionally, two modes of neck retraction are distinguished within extant turtles. Cryptodires retract the neck in a vertical plane within the carapace (Fig. 1A), whereas pleurodires fold their neck horizontally under the anterior edge of the shell (Fig. 1B) (Herrel et al., 2008). Recently, stem turtles were inferred to have been able to retract their neck by tucking it under the anterior part of the shell, similar to pleurodires (Werneburg et al., 2015a) (Fig. 1C). Compared to stem turtles, however, pleurodires have elongated necks and an additional loop of the retracted neck to the other body side is needed to fully pack it under the shell. Therefore, an S-shaped neck curve can be observed in pleurodires (Fig. 1B). Also cryptodires have elongated necks when compared to the ancestral condition and an S-shape of the neck is also present when their neck is retracted (Fig. 1A).

The neck retraction mode of stem turtles apparently represented just a modified lateral flexion of the neck (Werneburg et al., 2015a). Therefore, during retraction, intervertebral rotation of the cervical vertebrae was performed.

The pleurodiran neck retraction was directly derived from the ancestral mode of retraction. Particularly only the middle third of the cervical column was found to have been modified comprehensively in pleurodires in order to enable the loop of the elongated neck during retraction (Werneburg et al., 2015a,b). In pleurodires, the neck–body articulation between the eighth cervical and the first body vertebra did not experience much anatomical change when compared to stem turtles (Joyce, 2007; Werneburg et al., 2015b; Williams, 1950). To enable the neck loop, the last, namely the eighth cervical – and consequently also the posterior part of the whole neck – were simply flexed to the opposite body side during retraction of the head.

In contrast, the eighth cervical of cryptodires experienced several modifications (Werneburg et al., 2015b; Williams, 1950). It flexed about 180° when compared to the ancestral condition. In that way, the whole neck can be swung inside the body (Dalrymple, 1979).

The cryptodiran mode of retraction was recently hypothesized to be derived from the ancestral mode of dorsal neck flexion (i.e., dorsal neck bending). This conclusion was based on similar angular interrelationships that have been detected between cervical vertebrae during dorsal neck flexion in cryptodires and when the neck is retracted (Werneburg et al., 2015a). Alternatively, similar to the pleurodiran retraction, Werneburg et al. (2015b) hypothesized, by assessing comparative vertebral anatomy, that the cryptodiran retraction was also derived from the already established mode of retraction found in stem turtles. In that case, the ancestrally retracted neck would have been rotated intervertebrally through evolution in order to move from a diagonal rotation (stem turtles) towards the sagittal orientation found in the retracted necks of cryptodires. These contested hypotheses on the origin of cryptodiran neck retraction – either the ancestral dorsal flexion or

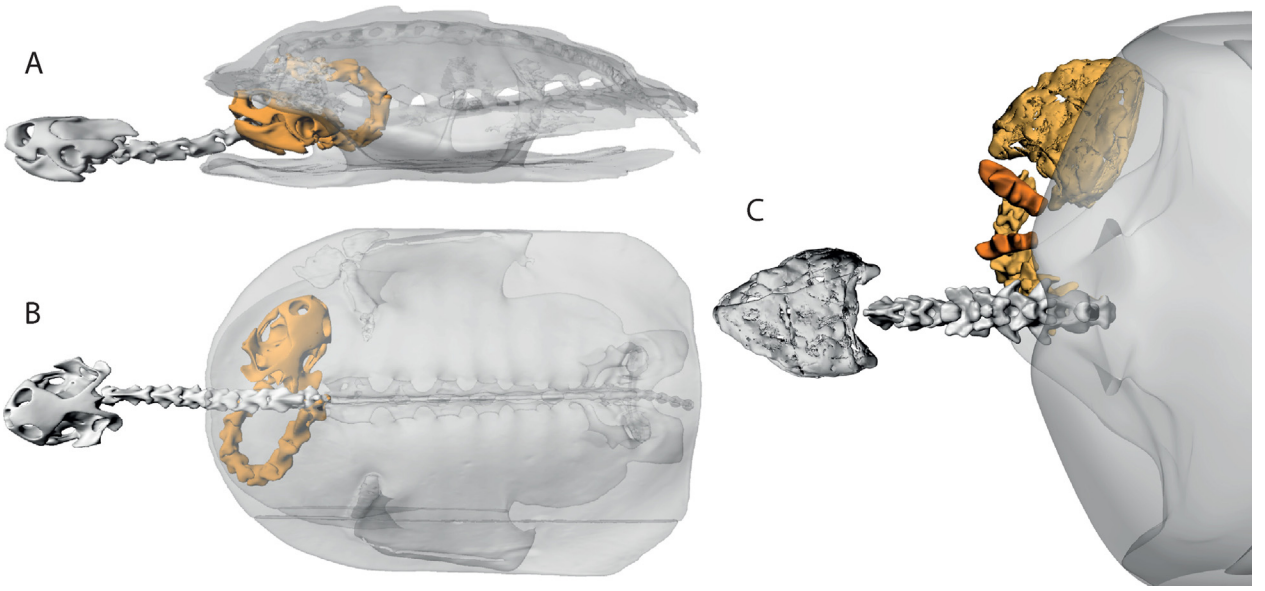

Fig. 1. (Color online.) Types of neck retraction in Testudinata. **A**. An extant cryptodire turtle, *Graptemys pseudogeographica*, in lateral view, (**B**) an extant pleurodire turtle, *Phrynops hilarii*, in dorsal view, **(C)** the stem turtle *Proganochelys quenstedti* in dorsal view. Gray neck/head = extended neck position, orange = retracted neck position, dark orange = osteoderms on the neck. Shells are shown transparent. Artwork by Juliane Hinz (Tübingen) and I.W.
Fig. 1. (Couleur en ligne.) Types de rétraction du cou chez les Testudinata. **A**. Tortue cryptodire actuelle, *Graptemys pseudogeographica*, en vue latérale**,** (**B**) tortue pleurodire actuelle, *Phrynops hilarii*, en vue dorsale, (**C**) tortue souche *Proganochelys quenstedti* en vue dorsale. Gris cou/tête = position du cou en extension, orange = position du cou rétracté, orange foncé = ostéodermes sur le cou. Les carapaces sont montrées en transparence. Iconographie de Juliane Hinz (Tübingen) et I.W.

the lateral tucking as a precursor – require further exploration.

Kilias (1957) suggested a tentative correlation between the mode of neck retraction and the shape of the temporal skull region in turtles (reviewed by Werneburg, 2012). Roughly, two major types of marginal reduction can be distinguished in the dermal skull wall, namely, the posterodorsal ("occiput") and the anteroventral ("cheek") emargination. Kilias (1957) primarily correlated the former to the cryptodiran mode of retraction, whereas the latter would be correlated to the pleurodiran mode. Thereby, both types of marginal skull reductions would occur respectively in order to better fit the retracted head within the confines of the shell and shoulder girdle and their related soft tissue. It is worth mentioning, however, that both types of emargination – to a different extent – are found to occur simultaneously in most turtles. This fact strongly suggests that other factors also influence the shaping of the temporal skull region in turtles (Werneburg, 2012) – not neck retraction alone. Moreover, whether there is a clear correlation between the mode of retraction and the reduction of temporal bones, and how this relates to the fossil record, was never tested.

Using a geometric morphometric approach, I compare the shapes of the turtle necks at different positions of their motion. Therefore, seven to ten coordinates (landmarks) of the neck were measured in every species and for six types of neck positions separately. I estimated which neck motion could be derived from one another and how the shape parameters of the retracted necks are related to the types of skull emargination. The findings of the present study and the cranial plasticity justify a reassessment of the hypothesis of an ancestry of the anapsid morphotype of the turtle skull (i.e., without any internal temporal opening) in relation to neck motion.

2. Methods

2.1. Documentation of neck shapes

Neck shape was documented for different positions of neck motion (Fig. 2A–B). Therefore, photographs of manually articulated necks as well as necks in life condition were compared. In addition to illustrations from older literature, I used the recent data of Werneburg et al. (2015a), who made medical CT-scans and fluoroscopy of neck motion in living specimens (Table 1). In total, the neck mobility of 39 turtle and two squamate species (as outgroup) were analyzed (Table 1, S4) by measuring angles between adjacent vertebrae. Werneburg et al. (2015a) also calculated and simulated life mobility in the fossil stem turtle *Proganochelys quenstedti* (Staatliches Museum für Naturkunde Stuttgart; SMNS 16980). The neck positions of this species, as reconstructed by those authors, were used herein to infer the ancestral shape of neck curves.

The following neck positions were documented for each species separately: the maximal (A) dorsal, (B) ventral, and (C) lateral neck flexion (i.e., bending of the neck); (D) the maximal extended neck position; (E) the neutral neck position (i.e., full overlap of articular facets of the adjacent zygapophyses); and (F) the neck positions during maximal retraction (Fig. 2A–B). Using different imaging software (Amira 5.2.2., Meshlab v1.3.0, IrfanView 4.32), I generated screen shot pictures of those neck positions. All

Table 1
Specimens analyzed. EQs rounded to three decimal places. Image references for EQ-calculation: The Berlin specimen of †*Proganochelys quenstedti* (*) was not used for EQ-calculation because the skull is largely deformed (Gaffney, 1990).
Tableau 1
Spécimens analysés. EQs arrondis à la troisième décimale. Références d'image pour le calcul d'EQ : le spécimen Berlin de *Proganochelys quenstedti* (*) n'a pas été utilisé pour le calcul d'EQ, car le crâne est très déformé (Gaffney, 1990).

Species (specimens/treatments)	Imaging method	Reference	EQav	EQpd	Image reference for EQ-calculation
Pogona vitticeps	CT	IW1134, Tiergarten Schönbrunn	–	–	–
Pogona vitticeps	Fluoroscopy	IW1134, Tiergarten Schönbrunn	–	–	–
Rhacodactylus cilliatus	CT	IW1136, Tiergarten Schönbrunn	–	–	–
†*Chisternon undatum*	Photo	IW922 (ANMH 5904)	0.424	0.619	Gaffney (1979)
†*Meiolania platyceps (1)*	Photo	Gaffney (1985)	0	0	Gaffney (1983)
†*Meiolania platyceps (2)*	Photo	IW924A (AMNH 57984)	Dito	Dito	Dito
†*Naomichelys speciosa*	Photo	IW931 (FNMH PR273)	0.137	0.217	This study
†*Proganochelys quenstedii (1)*	Photo	IW921A (cast of Stuttgart specimen SMNS16980)	0.067	0.102	This study
†*Proganochelys quenstedii (2)*	Photo	(Gaffney, 1990): Museum Berlin specimen MB1910.45.2	Dito	Dito	This study*
†*Proganochelys quenstedii (3)*	Photo	Gaffney (1990): Stuttgart specimen SMNS16980	Dito	Dito	This study
†*Proganochelys quenstedii (4)*	Simulation	Werneburg et al., 2015a; SMNS16980	Dito	Dito	This study
†*Proganochelys quenstedii (5), lateral retraction*	Simulation	Werneburg et al., 2015a; SMNS16980	Dito	Dito	This study
Apalone spinifera (1)	CT	Herrel et al., 2008	0.251	2.827	Dalrymple (1975)
Apalone spinifera (2)	Drawing	Dalrymple (1979)	0.281	Dito	Dalrymple (1979) [labeled as "tionychid"] dito
Astrochelys radiata	CT	IW1133, Tiergarten Schönbrunn	0.501	1.651	This study
Carettochelys insculpta	Photo	IW919 (SMF56626)	0.431	1.872	This study
Chelodina longicollis (1)	Fluoroscopy	Herrel et al. (2008) (breathing)	1.752	0	Van Damme and Aerts (1997)
Chelodina longicollis (2)	Drawing	Herrel et al. (2008)	Dito	Dito	Dito
Chelodina novaeguinaeae	Fluoroscopy	IW, courtesy Josef Weisgram	Dito	Dito	Data for *C. longicollis* used
Chelonoidis nigra	CT	IW1162, Tiergarten Schönbrunn	0.636	0.528	This study: SMF 67582: *Chelonoidis* sp.
Chelydra serpentina (1)	Photo	IW933 (SMF32846)	0.290	1.402	This study
Chelydra serpentina (2)	CT	IW1115, Tiergarten Schönbrunn	0.313	1.388	This study
Chelydra serpentina (3)	Fluoroscopy	IW1115, Tiergarten Schönbrunn	0.313	1.388	This study
Chrysemys picta	Fluoroscopy	Scanlon (1982)	0.484	1.745	Jamniczky and Russell (2007)
Cuora ("Cyclemys") mouhotii	Photo	IW939 (SMF71599)	0.526	2.307	This study
Dermatemys mawii	Photo	IW1035 (SMF59463)	0.328	1.492	This study
Emys orbicularis (1)	Photo	IW937 (SMF68814)	0.530	1.889	This study
Emys orbicularis (2)	CT	IW1135, Tiergarten Schönbrunn	0.433	1.534	This study
Emys orbicularis (3)	Fluoroscopy	IW1135, Tiergarten Schönbrunn	Dito	Dito	This study
Emys orbicularis (4)	Fluoroscopy	IW1116, Joseph Weisgram lab. Vienna/Austria	Dito	Dito	This study
Erymnochelys madagascariensis	Photo	IW1048 (SMF7979)	0.378	0.150	This study
Geochelone pardalis	CT	IW1164, Tiergarten Schönbrunn	0.670	1.876	This study
Graptemys pseudogeographica (1)	CT	IW1137, Tiergarten Schönbrunn	0.552	0.434	This study
Graptemys pseudogeographica (2)	Fluoroscopy	IW1137, Tiergarten Schönbrunn	Dito	Dito	This study
Graptemys pseudogeographica (3)	CT	IW1138, Tiergarten Schönbrunn	0.536	2.147	This study
Graptemys pseudogeographica (4)	Fluoroscopy	IW1138, Tiergarten Schönbrunn	Dito	Dito	This study
Hydromedusa tectifera	Photo	IW1040 (SMF70500)	0.623	0.336	This study
Hyosemys grandis (1)	CT	IW1139, Tiergarten Schönbrunn	0.648	1.80	This study
Hyosemys grandis (2)	Fluoroscopy	IW1118, Tiergarten Schönbrunn	Dito	Dito	This study
Indotestudo elongata	Photo	IW1034 (SMF71585)	0.526	1.871	This study
Kinixys erosa	Photo	IW1044 (SMF40166)	0.446	2.279	This study
Kinosternon scorpioides	Photo	IW936 (SMF71893)	0.141	1.771	This study
Kinosternon subrubum	Drawing	Bramble et al. (1984)	0.156	0.461	Gaffney (1979)
Macrochelys temmincki	Photo	IW1113 (TCT)	0.222	0.765	This study
Malacochersus tornieri (1)	CT	IW1142, Tiergarten Schönbrunn	0.640	1.832	This study
Malacochersus tornieri (2)	Fluoroscopy	IW1119, Tiergarten Schönbrunn	Dito	Dito	Dito
Melaclemys ("centrata") terrapin	Photo	IW934 (SMF36419)	0.453	0.557	This study
Pelodiscus sinensis	CT	IW1163, Michaela Gumpenberger lab, Vienna	3.592	5.022	This study
Pelomedusa subrufa	Fluoroscopy	IW1167, Joseph Weisgram lab, Vienna/Austria	0.464	1.350	Gaffney (1979)
Phrynops geoffroanus	Photo	IW935 (SMF45470)	1.364	0.665	This study

Table 1 (*Continued*)

Species (specimens/treatments)	Imaging method	Reference	EQav	EQpd	Image reference for EQ-calculation
Phrynops hilarii (1)	CT	IW1140, Tiergarten Schönbrunn	1.496	0.685	This study
Phrynops hilarii (2)	Fluoroscopy	IW1140, Tiergarten Schönbrunn	Dito	Dito	This study
Phrynops hilarii (3)	Fluoroscopy	IW1121, Tiergarten Schönbrunn	Dito	Dito	Dito
Platysternon megacephalon (1)	CT	IW1165, Michaela Gumpenberger lab, Vienna	0.091	0.881	This study, Gaffney (1979)
Platysternon megacephalon (2)	Photo	IW920 (SMF69484)	Dito	Dito	This study
Podocnemis unifilis (1)	CT	IW1141, Pet trade	0.670	1.164	This study
Podocnemis unifilis (2)	Fluoroscopy	IW1141, Pet trade	Dito	Dito	Dito
Podocnemis unifilis (3)	Photo	IW932 (SMF55470)	0.669	0.938	This study
Pyxis ("Acinixys") planicauda	Photo	IW1033 (SMF7722)	0.767	1.697	This study
Sternotherus carinatus (1)	CT	IW1145, Pet trade	0.215	1.931	This study
Sternotherus carinatus (2)	Fluoroscopy	IW1145, Pet trade	Dito	Dito	This study
Terrapene carolina	Photo	Landberg et al. (2003)	0.474	0.511	Landberg et al. (2003), Legler (1960)
Testudo graeca (1)	CT	IW1143, Tiergarten Schönbrunn	0.604	1.638	This study
Testudo graeca (2)	Photo	IW1043 (SMF67588)	Dito	Dito	This study
Testudo hermanni (1)	CT	IW1130, Michaela Gumpenberger lab, Vienna	0.721	2.177	This study
Testudo hermanni (2)	CT	IW1144, Tiergarten Schönbrunn	Dito	Dito	This study
Testudo hermanni (3)	Photo	IW1045 (SMF71882)	0.599	2.421	This study
Testudo hermanni (4)	Fluoroscopy	Weisgram and Splechtna (1990)	Dito	Dito	This study
Trachemys scripta (1)	CT	IW1131, Michaela Gumpenberger lab, Vienna	0.506	2.171	This study
Trachemys scripta (2)	Photo	Callister et al. (2005)	Dito	Dito	This study

necks at lateral flexion and the retracted necks of the stem turtle and pleurodires were photographed in a ventral planar view of the necks. All other neck positions were photographed in a lateral planar view (Fig. 2B).

2.2. Landmark data

Tps-files, which refer to image folders, were created using the software TpsUtil. Using TpsDig2, the most ventral and medial points in the centrals' articulations were defined as homologous landmarks in fossil and extant material (Fig. 2Bc–i, Table 2). Each neck motion was measured separately in each species. In extant specimens and in the fossil *P. quenstedti*, the articulation between skull and neck and the anteroventral most point of the upper jaw were scored correspondingly (Fig. 2Ba–b). For other fossils, no skulls were available and only the landmarks between the vertebrae were measured (Fig. 2Bc–i). The various pieces of software used are available at http://life.bio.sunysb.edu/morph/

Table 2
Definition of landmarks of the neck curve. Compare to Fig. 1.
Tableau 2
Définition des repères de courbure du cou. À comparer avec la Fig. 1.

#	Description
a	Anteroventral tip of the snout
b	Ventral articulation point between skull and cervical vertebrae 1
c	Ventral articulation point between cervical vertebrae 1 and cervical vertebrae 2
d	Ventral articulation point between cervical vertebrae 2 and cervical vertebrae 3
e	Ventral articulation point between cervical vertebrae 3 and cervical vertebrae 4
f	Ventral articulation point between cervical vertebrae 4 and cervical vertebrae 5
g	Ventral articulation point between cervical vertebrae 5 and cervical vertebrae 6
h	Ventral articulation point between cervical vertebrae 6 and cervical vertebrae 7
i	Ventral articulation point between cervical vertebrae 7 and cervical vertebrae 8
j	Ventral articulation point between cervical vertebrae 8 and dorsal (thoracal) vertebrae 1

2.3. Geometric morphometrics of neck/head curves

Using the software PAST 2.15 (Hammer et al., 2001), 2D-geometric morphometric analyses were performed to characterize the shapes of the neck/head curves. To remove translation, rotation, and size effects, the Generalized Procrustes method (Rohlf and Slice, 1990) was used, which normalizes the coordinates of the landmark data with the help of a calculated centroid. Principal component analyses (PCA) were performed (Figs. 3 and 4, S1–16). Eigen values and percent variance of each analysis (Table 3) as well as PC1 scores and the normalized size of each curve (Table 4) were documented.

2.4. Emargination quotients

For each species, the relative sizes of emargination (depth divided by breadth) were documented and named as "emargination quotients" (EQs) (Table 1, Fig. 5). Depths and breadths of the emarginations were measured in planar lateral skull view for anteroventral emargination (Fig. 5A) and in planar dorsal skull view for posterodorsal emargination (cf., Fig. 5B).

The EQs describe the relative expansion of the respective emarginations. The length of the anteroventral emargination is measured between the posteroventralmost point of the upper jaw and, following a straight line, the ventralmost point of the ear capsule. From the middle point of this line, a straight line was measured to the

Table 3
Eigenvalues (EV) and percent variance (%) of the principal component analyses of this study for the respective data sets including all species. Principal components (PC) 1 to 20 are listed. Compare to the figures listed in the table.
Tableau 3
Valeurs propres (EV) et variance en pourcent (%) des analyses en composantes principales pour les groupes respectifs de données incluant toutes les espèces. Les composantes principales (PC) de 1 à 20 sont listées. À comparer avec les figures listées sur le tableau.

PC	EV	%	EV	%	EV	%	EV	%	EV	%	EV	%	EV	%	EV	%	EV	%
Figure	3 and S1		4 and S2		S3–S4		S5–S6		S7–S8		S9–S10		S11–S12		S13–S14		S15–S16	
Data set	All data. 7 landmarks		Retractions. 7 landmarks		Neutral		Extended		Dorsal		Ventra1		Pleurodire retracted. lateral		Retracted. Cryptodira		All data. extant species	
1	0.056155	76.3	0.019868	49.682	0.017749	88.782	0.0151162	60.692	0.0467114	62.636	0.0174786	45.864	0.0847586	72.418	0.0427448	64.343	0.108144	71.99
2	0.006782	9.2155	0.010965	27.419	0.000822	4.1107	0.00515258	20.688	0.0195789	26.254	0.0134137	35.198	0.0154692	13.217	0.011681	17.583	0.0174689	11.629
3	0.005075	6.8952	0.003331	8.3295	0.000561	2.8038	0.00198684	7.9772	0.00356721	4.7833	0.00424014	11.126	0.00733271	6.2651	0.00432019	6.5031	0.0112374	7.4806
4	0.00216	2.9346	0.00283	7.0762	0.000304	1.5229	0.00128511	5.1598	0.00254702	3.4153	0.00107508	2.821	0.00382503	3.2681	0.0025408	3.8246	0.00639058	4.2542
5	0.001784	2.4233	0.001102	2.7544	0.000174	0.86918	0.000532978	2.1399	0.00074473	0.99862	0.000830413	2.179	0.00228728	1.9543	0.00231471	3.4843	0.00314295	2.0922
6	0.000567	0.77012	0.00076	1.9013	0.000127	0.63324	0.000304746	1.2236	0.000557755	0.7479	0.000458957	1.2043	0.00130298	1.1133	0.00122594	1.8454	0.00135023	0.89884
7	0.000411	0.55806	0.000364	0.90931	9.23×10^{-5}	0.46173	0.000189284	0.75998	0.000366587	0.49156	0.000234645	0.61571	0.00098219	0.83919	0.000595242	0.896	0.00117941	0.78513
8	0.000223	0.3024	0.000286	0.71584	7.54×10^{-5}	0.37741	0.000123893	0.49743	0.000198623	0.26634	0.000152677	0.40063	0.00043559	0.37217	0.000344809	0.51903	0.00038008	0.25302
9	0.000202	0.27501	0.000205	0.51352	4.52×10^{-5}	0.22622	9.69×10^{-5}	0.38907	6.13×10^{-5}	0.11654	0.000114369	0.3001	0.00026087	0.22289	0.000191332	0.28801	0.00023339	0.15537
10	0.000141	0.1917	0.000178	0.44419	2.99×10^{-5}	0.14947	4.05×10^{-5}	0.16243	6.13×10^{-5}	0.10851	6.13×10^{-5}	0.16082	0.00013959	0.11927	0.000132949	0.20012	0.00019963	0.13289
11	9.91×10^{-5}	0.13464	0.000102	0.2548	1.26×10^{-5}	0.062847	3.37×10^{-5}	0.13538	6.13×10^{-5}	0.081984	2.82×10^{-5}	0.073957	6.62×10^{-5}	0.056522	0.000109282	0.1645	1.25×10^{-4}	0.082926
12	5.80×10^{-16}	7.88×10^{-13}	6.27×10^{-16}	1.57×10^{-12}	6.27×10^{-16}	3.13×10^{-12}	2.09×10^{-5}	0.084108	6.13×10^{-5}	0.039486	1.10×10^{-5}	0.028872	6.36×10^{-5}	0.054318	8.36×10^{-5}	0.12582	1.06×10^{-4}	0.07081
13	3.64×10^{-16}	4.94×10^{-13}	3.01×10^{-16}	7.53×10^{-13}	2.22×10^{-16}	1.11×10^{-12}	1.22×10^{-5}	0.048975	6.13×10^{-5}	0.030982	6.27×10^{-6}	0.016461	5.83×10^{-5}	0.04982	6.60×10^{-5}	0.099302	7.20×10^{-5}	0.047906
14	2.44×10^{-16}	3.3×10^{-13}	1.82×10^{-16}	4.56×10^{-13}	1.10×10^{-16}	5.48×10^{-13}	5.88×10^{-6}	0.023594	6.13×10^{-5}	0.019487	4.46×10^{-6}	0.0117	2.85×10^{-5}	0.024347	3.37×10^{-5}	0.05073	6.67×10^{-5}	0.044403
15							2.44×10^{-6}	0.0098149	6.13×10^{-6}	0.0077096			1.87×10^{-5}	0.016	2.09×10^{-5}	0.031474	6.46×10^{-5}	0.043036
16							1.84×10^{-6}	0.0073696	6.13×10^{-6}	0.0023856			7.55×10^{-6}	0.0064502	1.50×10^{-5}	0.022615	3.85×10^{-5}	0.025641
17							4.18×10^{-5}	0.0016785	6.13×10^{-7}	0.00026045			3.20×10^{-6}	0.0027358	1.29×10^{-5}	0.019475	2.08×10^{-5}	0.01387
18							4.54×10^{-17}	1.82×10^{-13}	6.13×10^{-17}	8.57×10^{-14}			1.27×10^{-16}	1.09×10^{-13}	4.39×10^{-16}	6.61×10^{-13}	4.74×10^{-16}	3.16×10^{-13}
19									6.13×10^{-17}	6.13×10^{-14}			5.72×10^{-17}	4.88×10^{-14}	2.00×10^{-16}	3.01×10^{-13}	3.86×10^{-16}	2.57×10^{-13}
20													1.45×10^{-17}	1.24×10^{-14}	1.12×10^{-16}	1.69×10^{-13}	2.77×10^{-16}	1.84×10^{-13}

Table 4
Shape parameters (PC1, normalized centroid size) for different neck positions (excluding outgroup).
Tableau 4
Paramètres de forme (PCI, taille centroïde normalisée) pour différentes positions du cou (à l'exclusion de l'*outgroup*).

Species	(A) Score of PC1-axis							(B) Centroid size (normalized)						
Neck position	Dorsal	Ventral	Lateral	Extended	Normal	Pleurodiran retracted	Cryptodiran retracted	Dorsal	Ventral	Lateral	Extended	Normal	Pleurodiran retracted	Cryptodiran retracted
†*Chisternon undatum*	–	–	–	–	0.23221	–	–	–	–	–	–	0.370835	–	–
†*Meiolania platyceps (1)*	–	–	–	–	0.10006	–	–	–	–	–	–	0.379303	–	–
†*Meiolania platyceps (2)*	–	–	–	–	0.13702	–	–	–	–	–	–	0.377895	–	–
†*Naomichelys speciosa*	–	–	–	–	0.17237	–	–	–	–	–	–	0.375782	–	–
†*Proganochelys quenstedii (1)*	–	–	–	–	0.2132	–	–	–	–	–	–	0.372348	–	–
†*Proganochelys quenstedii (2)*	–	–	–	–	0.19894	–	–	–	–	–	–	0.373402	–	–
†*Proganochelys quenstedii (3)*	–	–	–	–	0.20555	–	–	–	–	–	–	0.373232	–	–
†*Proganochelys quenstedii (4)*	0.33204	−0.007182	−0.041059	–	–	–	–	0.29994	0.317764	0.317634	–	–	–	–
†*Proganochelys quenstedii (5). lateral retraction*	–	–	−0.12442	–	–	–	–	–	–	0.312662	–	–	–	–
Apalone spinifera (1)	–	–	–	−0.037854	–	–	−0.015958	–	–	–	0.312111	–	–	0.3173
Apalone spinifera (2)	–	–	–	–	–	–	−0.11676	–	–	–	–	–	–	0.31225
Astrochelys radiata	–	–	–	–	–	–	−0.10678	–	–	–	–	–	–	0.32286
Carettochelys insculpta	–	–	–	–	−0.095844	–	–	–	–	–	–	0.379722	–	–
Chelodina longicollis (1)	0.22016	–	–	0.13817	–	–	–	0.313154	–	–	–	–	–	–
Chelodina longicollis (2)	0.23382	−0.041566	–	–	–	–	–	0.31304	0.31702	–	–	–	–	–
Chelodina novaeguinaeae	–	–	–	–	–	0.074302	–	–	–	–	–	–	0.318184	–
Chelonoidis nigra	–	–	–	–	–	–	0.37985	–	–	–	–	–	–	0.29616
Chelydra serpentina (1)	–	–	–	–	0.019908	–	–	–	–	–	–	0.381332	–	–
Chelydra serpentina (2)	–	–	–	–	–	–	0.26974	–	–	–	–	–	–	0.31268
Chelydra serpentina (3)	–	–	–	–	–	–	0.1053	–	–	–	–	–	–	0.32149
Chrysemys picta	0.10585	–	–	–	–	–	0.033126	0.320583	–	–	–	–	–	0.32435
Cuora ("Cyclemys") mouhotii	–	–	–	–	−0.12537	–	–	–	–	–	–	0.378503	–	–
Dermatemys mawii	–	–	–	–	−0.078071	–	–	–	–	–	–	0.380147	–	–
Emys orbicularis (1)	–	–	–	–	−0.12753	–	–	–	–	–	–	0.378188	–	–
Emys orbicularis (2)	–	–	–	–	–	–	−0.16843	–	–	–	–	–	–	0.32176
Emys orbicularis (3)	–	0.089973	0.12909	–	–	–	–	–	0.31846	0.317573	–	–	–	–
Emys orbicularis (4)	–	–	−0.026654	–	–	–	–	–	–	0.320889	–	–	–	–
Erymnochelys madagascariensis	–	–	–	–	0.045123	–	–	–	–	–	–	0.38086	–	–
Geochelone pardalis	–	–	–	–	–	–	0.39407	–	–	–	–	–	–	0.29485
Graptemys pseudogeographica (1)	−0.18733	−0.16353	−0.041014	−0.067338	–	–	−0.24593	0.317077	0.315025	0.319918	0.316639	–	–	0.31385
Graptemys pseudogeographica (2)	0.10689	0.10002	−0.02636	0.018563	–	–	–	0.320642	0.317799	0.322181	0.317839	–	–	–
Graptemys pseudogeographica (3)	−0.038777	−0.14445	−0.021148	−0.053487	–	–	−0.14052	0.320324	0.316209	0.318122	0.316889	–	–	0.32353
Graptemys pseudogeographica (4)	–	–	0.0074368	–	–	–	–	–	–	0.319253	–	–	–	–
Hydromedusa tectifera	–	–	–	–	0.046339	–	–	–	–	–	–	0.38108	–	–
Hyosemys grandis (1)	–	–	–	–	–	–	−0.1529	–	–	–	–	–	–	0.32154
Hyosemys grandis (2)	–	–	–	–	–	–	−0.046789	–	–	–	–	–	–	0.32248
Indotestudo elongata	–	–	–	–	−0.11567	–	–	–	–	–	–	0.377937	–	–
Kinixys erosa	–	–	–	–	−0.17692	–	–	–	–	–	–	0.375116	–	–
Kinosternon scorpioides	–	–	–	–	−0.19559	–	–	–	–	–	–	0.3739	–	–
Kinosternon subrubum	–	–	–	–	–	–	−0.18307	–	–	–	–	–	–	0.32122
Macrochelys temmincki	–	–	–	–	−0.13789	–	–	–	–	–	–	0.377721	–	–
Malacochersus tornieri (1)	0.075957	−0.11853	0.057987	0.024274	–	–	−0.048719	0.319757	0.315912	0.317551	0.316485	–	–	0.32462
Malacochersus tornieri (2)	–	–	–	–	–	–	0.13184	–	–	–	–	–	–	0.31836
Melaclemys ("centrata") terrapin	–	–	–	–	−0.1042	–	–	–	–	–	–	0.379049	–	–
Pelodiscus sinensis	–	–	–	–	–	–	0.17642	–	–	–	–	–	–	0.31254
Pelomedusa subrufa	–	–	–	–	–	0.061216	–	–	–	–	–	–	0.31813	–
Phrynops geoffroanus	–	–	–	–	0.12302	–	–	–	–	–	–	0.378617	–	–
Phrynops hilarii (1)	0.13496	–	0.073582	0.10953	–	0.080542	–	0.320047	–	–	–	–	0.31633	–
Phrynops hilarii (2)	−0.079674	−0.009903	–	0.077425	–	0.0063498	–	0.321511	0.319453	–	0.316856	–	–	–
Phrynops hilarii (3)	–	–	−0.072638	0.06708	–	–	–	–	–	0.319948	0.316794	–	0.318362	–
Platysternon megacephalon (1)	–	–	–	–	–	–	5.24×10^{-1}	–	–	–	–	–	–	0.26682
Platysternon megacephalon (2)	–	–	–	–	−0.13334	–	–	–	–	–	–	0.377232	–	–

Table 4 (*Continued*)

Species	(A) Score of PC1-axis							(B) Centroid size (normalized)						
Neck position	Dorsal	Ventral	Lateral	Extended	Normal	Pleurodiran retracted	Cryptodiran retracted	Dorsal	Ventral	Lateral	Extended	Normal	Pleurodiran retracted	Cryptodiran retracted
Podocnemis unifilis (1)	–0.00029719	–0.00387	0.08197	0.1155	–	–	–	0.322278	0.316684	0.317226	0.315219	–	–	–
Podocnemis unifilis (2)	–	–	0.33826	–	–	–0.22241	–	–	–	0.297898	–	–	0.310054	–
Podocnemis unifilis (3)	–	–	–	–	0.061984	–	–	–	–	–	–	0.380691	–	–
Pyxis ("Acinixys") planicauda	–	–	–	–	–0.021329	–	–	–	–	–	–	0.380825	–	–
Sternotherus carinatus (1)	–0.2962	0.016875	–0.28164	–0.10497		-	–0.18335	0.301056	0.317386	0.30677	0.316101	–	–	0.32052
Sternotherus carinatus (2)	–0.12655	0.1389	–	–0.084856		–	–0.085439	0.320201	0.316122	–	0.316217	–	–	0.32507
Terrapene carolina	–	–	–	–	–0.080405	–	–0.23281	–	–	–	–	0.380084	–	0.31312
Testudo graeca (1)	–0.1058	0.27691	0.099763	–0.011684	–	–	–0.09674	0.320641	0.30648	0.319324	0.317942	–	–	0.32413
Testudo graeca (2)	–0.069226	–	–	–	–0.1054	–	–0.123	–	–	–	–	0.379299	–	–
Testudo hermanni (1)	–	–	–0.034677	–0.026225	–	–	–	–	–	0.319765	0.317627	–	–	–
Testudo hermanni (2)	–0.006788	–0.13365	0.034189	–0.029149	–	–	–0.20306	0.32119	0.316459	0.313989	0.316521	–	–	0.31456
Testudo hermanni (3)	–	–	–	–	–0.011117	–	–	–	–	–	–	0.381296	–	–
Testudo hermanni (4)	–	–	–	–0.067531	–	–	–0.11571	0.320404	–	–	0.317268	–	–	0.32138
Trachemys scripta (1)	–0.29903	–	–0.15267	–0.067452	–	–	0.16287	0.302561	–	0.317618	0.316112	–	–	0.32088
Trachemys scripta (2)	–	–	–	–	–0.047053	–	0.088991	–	–	–	–	0.380336	–	0.32339

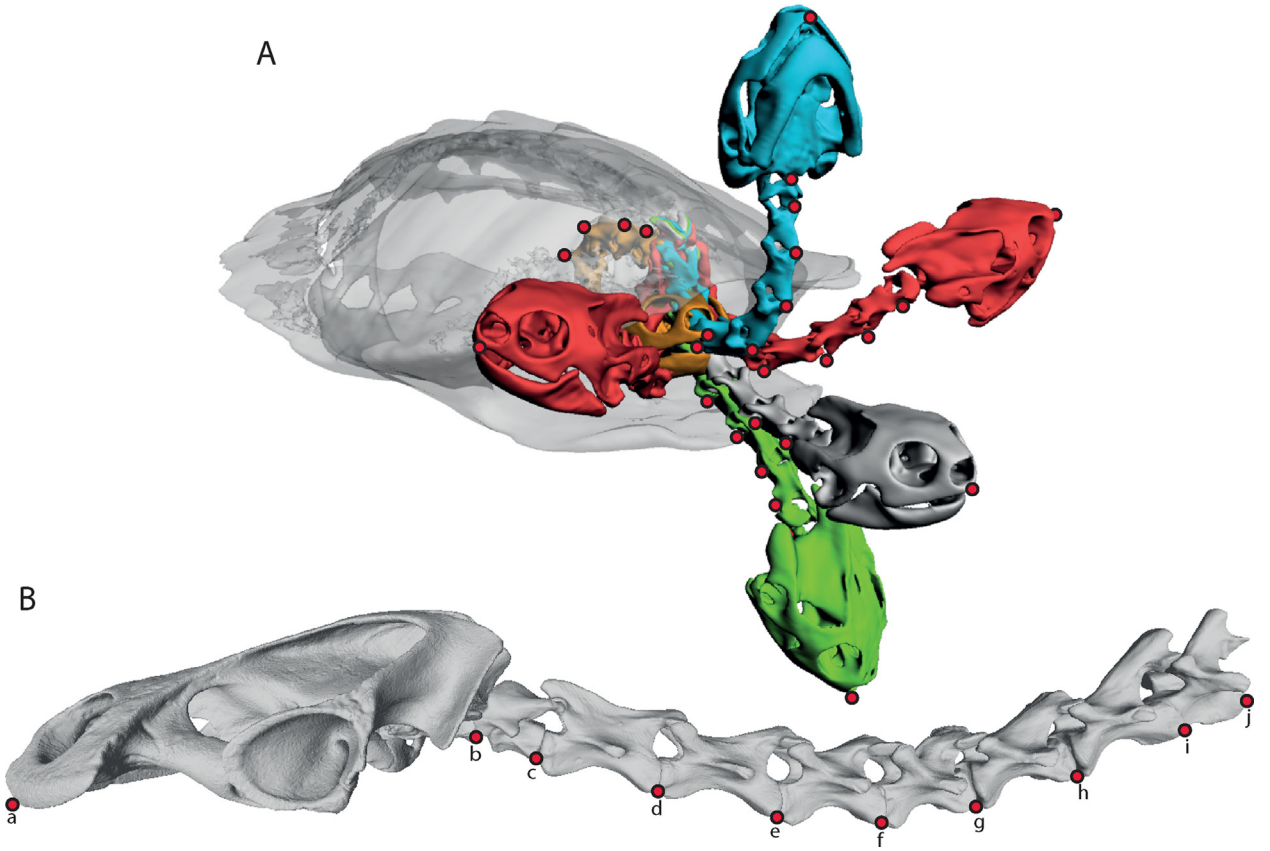

Fig. 2. (Color online.) Turtle neck positions and landmark definition. **A**. Computer-assisted tomography scans of different neck positions combined for a cryptodire turtle, *Malaclemys centrata*, in frontolateral perspective view: blue, maximal dorsal flexion; gray, extended neck position; green, maximal ventral flexion; red, maximal lateral flexion; orange, maximal retracted neck (see also Fig. 1). Indicated landmarks (red circles) correspond to B. **B**. Landmarks illustrated for the pleurodire *Phrynops geoffroanus* (#IW935; SMF45470). The neck is arranged in neutral position, i.e. the articular facets of the adjacent zygapophyses fully overlap. For all neck positions, landmarks were taken in a two-dimensional plane of the neck (as shown in Fig. 2B). For further descriptions, see Table 2 and text. Artwork by Juliane Hinz (Tübingen) and I.W.

Fig. 2. (Couleur en ligne.) Positions de cou de tortues et définition des repères. **A**. Scans CT de différentes positions de cou d'une tortue cryptodire *Malaclemys centrata*, en perspective frontolatéral e: en bleu, flexion dorsale maximale ; en gris, position du cou en extension ; en vert, flexion ventrale maximale ; en rouge, flexion latérale maximale ; en orange, cou en rétraction maximale (voir aussi Fig. 1). Les repères indiqués (points rouges) correspondent à B. **B**. Repères pour la tortue pleurodire *Phrynops geoffroanus* (1W935, SMF45470). Le cou est présenté en position neutre, c'est-à-dire que les facettes articulaires des zygapophyses adjacents se chevauchent complètement. Pour toutes les positions du cou, les repères ont été pris dans un plan bidimensionnel du cou (comme on peut le voir en Fig. 2B). Pour de plus amples descriptions, voir le Tableau 2 et le texte. Iconographie de Julian Hinz et I.W.

deepest overall expansion of the emargination (Fig. 5A). For the posterodorsal emargination, a straight line is measured between the posteriormost point of the supraoccipital crest and the posteriormost point of the squamosal crest (cf. Fig. 5B). From the middle point of this line, the depth of the emargination is measured towards the deepest most overall expansion of this emargination.

2.5. Neck curvature vs. emargination

For each species, EQs were compared to the neck curve shapes. For that, the EQs of anteroventral and posterodorsal emargination (Table 1) were correlated to the scores of PC1 (= largest shape variance; Table 4) of the respective neck curves (Table 5A–B). Centroid size of each curve was also compared to the EQs to estimate size correlations (Table 5C–D). Phylogenetic effect was corrected using phylogenetic independent contrast (Felsenstein, 1985) using the PDAP package in Mesquite 2.75 (Maddison and Maddison, 2011). A time scaled composite phylogeny of turtles was used as template (Fig. 6). Interrelationship of extinct taxa follows Werneburg et al. (2015b), interrelationship of extant taxa follows Thomson and Shaffer (2010), but the position of *Platysternon megacephalum* is that of Joyce et al. (2013). Divergence times of major turtle taxa follow Joyce et al. (2013) with adaptations by Werneburg et al. (2015b: caption of Table S9). Calibration numbers in million years (my) were rounded off to the nearest integer. For a non-calibrated node between two nodes of a known age, the branch lengths between the known ages were equally separated. Divergence times of specimens of the same species were defined as 1000 years. Specimens that were treated with different methods to detect neck shape were defined as terminal taxa and set into a polytomy (number of degrees of freedom to subtract for soft polytomies was set to 0).

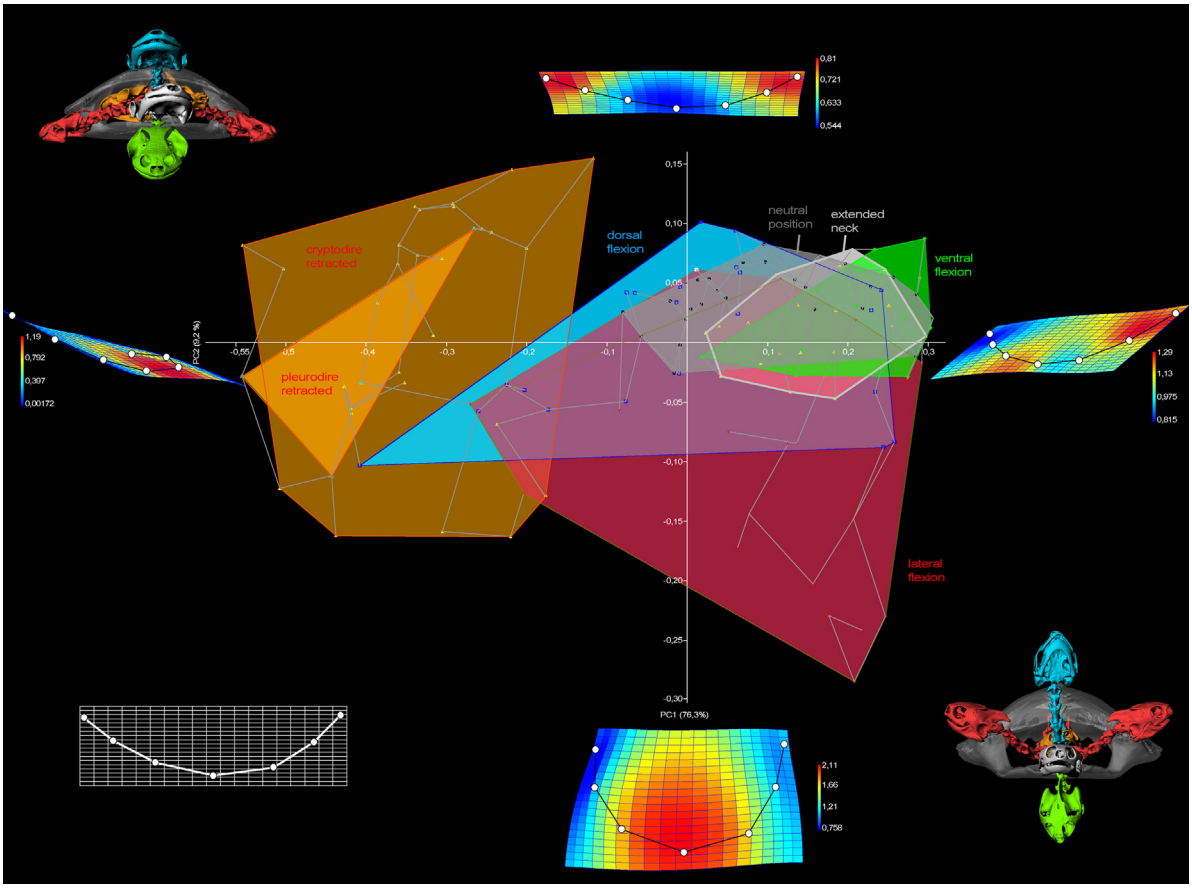

Fig. 3. (Color online.) Geometric morphometric analysis of the shape of the neck curves in extinct and extant species (Table 1). Principal component 1 and 2 are illustrated. Every point in the diagram represents the shape of one particular neck curve. For each species (for labelling see Fig. S1), dorsal, ventral, and lateral flexion, neutral neck position, and the extended and the retracted neck were measured. Convex hulls include all species' neck shapes for each motion separately. Seven landmarks, which describe the curvature of cervical one to eight, were used to generate shape parameters (see Fig. 2Bc–i). Bottom left: relative warp of the mean shape of all neck curves at point 0/0. Other relative warps refer to the shapes at the maximum labelled points of the PC-axes with colored expansion factors relative to the mean shape (see color code next to each relative warp). Frontal view of the pleurodire *Phrynops hilarii* (top left) and the cryptodire *Graptemys pseudogeographica* (right bottom) (modified from Werneburg et al., 2015a). Convex hulls labelled in the figure. Note the similar morphospace occupied by extended and neutral neck positions as well as pleurodiran and cryptodiran retraction. For detailed diagrams of PC1/2, PC2/3, PC1/3 see Fig. S1.

Fig. 3. (Couleur en ligne.) Analyse géométrique morphométrique de la forme des courbures du cou chez des espèces vivantes et éteintes (Tableau 1) Les composantes principales 1 et 2 sont ici illustrées. Chaque point du diagramme représente la forme de courbure d'un cou particulier. Pour chaque espèce (voir Fig. S1 pour le marquage), les flexions dorsale, ventrale et latérale, la position neutre du cou et l'extension et la rétraction du cou ont été mesurées. Chaque compartiment convexe inclut toutes les formes de cou des espèces pour chaque mouvement séparément. Sept repères qui décrivent la courbure des cervicales une à huit ont été utilisés pour générer des paramètres de forme (voir Fig. 2Bc–i). En bas à gauche : chaîne relative représentant la forme moyenne de toutes les courbures de cou au point 0/0. Les autres chaînes relatives se rapportent au maximum de points répertoriés sur les axes PC, avec les facteurs d'expansion relatifs à la forme moyenne colorés (voir le code couleur à côté de chaque chaîne relative). Vue frontale de tortues pleurodire *Phryniops hilarii* (en haut à gauche) et cryptodire *Graptemys pseudogeographica* (en bas à droite). Modifié d'après Werneburg et al., 2015a. Les compartiments convexes sont répertoriés sur la figure. À noter les « morphospaces » similaires occupés par les positions neutre et en extension du cou, de même que par la rétraction pleurodire et cryptodire. Pour les diagrammes détaillés de PC1/2, PC2/3, PC1/3, voir la Fig. S1.

2.6. Terminology and abbreviations

Anatomical terminology and abbreviations mainly follow Werneburg (2011, 2012, 2013a,b). **av** = anteroventral emargination (orange), **b** = breadth of an emargination in planar view, **cnubra-I and -II** = cornu branchiale I and II, **cpuhyo** = corpus hyoideus, **CV1**/-**2** = cervical vertebra 1 (atlas) and 2 (axis), **cstsprocc** = crista supraoccipitalis, **cstsqu** = crista squamosalis, **d** = depth of an emargination in planar view, **EQav/pd** = emargination quotient for anteroventral/posterodorsal skull emargination [i.e. depth divided by breadth of the emargination (see Fig. 5A)], **itf** = infratemporal fenestrum, **occ** = occipital region, **pd** = posterodorsal emargination (blue), **stf** = supratemporal fenestrum/cleft, **tym** = cavum tympanicum, **V** = ventral neck flexion.

2.7. Collections

Specimens are listed in Table 1. **AMNH** = American Museum of Natural History, New York, USA; **FMNH** = Field Museum of Natural History, Chicago, USA; **IW** = personal

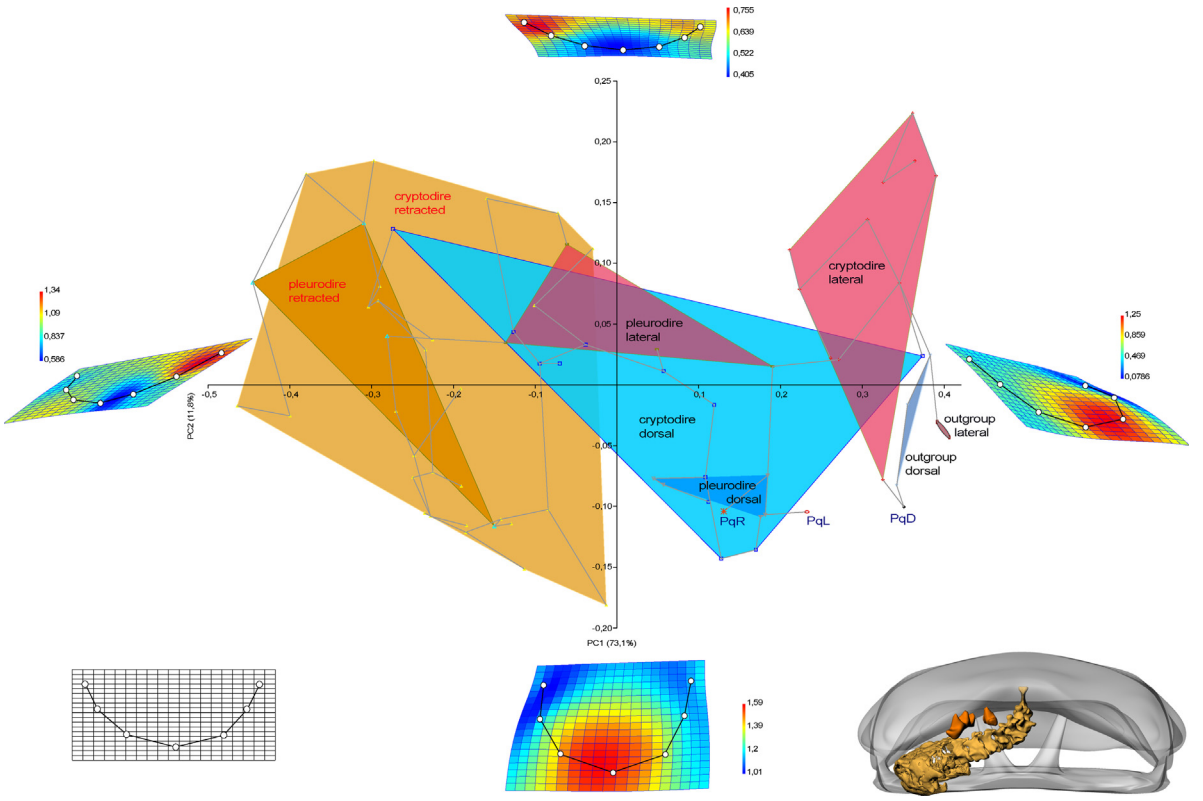

Fig. 4. (Color online.) Comparison of dorsal flexion, lateral flexion, and neck retraction curves. Principal component 1 and 2 are illustrated. For detailed diagrams of PC1/2, PC2/3, PC1/3 see Fig. S2. PqD/L/R = dorsal flexion (D)/lateral flexion (L)/lateral retraction (R) of the neck of *Proganochelys quenstedti*. Right lower corner shows *P. quenstedti* with its characteristically retracted neck (PqR) in frontal view as reconstructed by Werneburg et al. (2015a) ; compare to Fig. 1C.

Fig. 4. (Couleur en ligne.) Comparaison des courbes en flexion dorsale, en flexion latérale et en rétraction du cou. Les composantes principales 1 et 2 sont illustrées. Pour les diagrammes détaillés de PC1/2, PC2/3, PC1/3, voir la Fig. S2. PqD/L/R = flexion dorsale (D)/flexion latérale (L)/rétraction latérale (R) du cou de *Proganochelys quenstedti*. Dans le coin inférieur droit, on peut observer *P. quenstedti* avec son cou rétracté de manière caractéristique (PqR) en vue frontale, telle que l'ont reconstitué Werneburg et al. (2015a) ; à comparer avec la Fig. 1C.

Table 5
Pearson's correlation coefficients and *P*-value comparisons between neck shapes and emargination quotients of the phylogenetically independent contrast analysis. *r* = Pearson's correlation coefficients (= degree of linkage between two traits; if *r* = 1, complete correlation; if *r* = 0, no correlation), *P* = probability (if *P* = 1, *r* is not reliable; if *P* = 0, *r* is reliable; if *P* < 0.05, *r* is significant [indicated by *]).

Tableau 5
Coefficients de comparaison de Pearson et comparaisons des valeurs de *p* entre les formes du cou et les quotients d'émargination de l'analyse de contraste phylogénétiquement indépendant. *r* = coefficient de corrélation de Pearson (degré de liaison entre deux traits ; si *r* = 1, corrélation complète; si *r* = 0, pas de corrélation), *p* = probabilité (si *p* = 1, *r* n'est pas fiable ; si *p* = 0, *r* est fiable ; si *p* < 0,05, *r* est significatif [indiqué par *]).

	EQav		EQpd	
	r	*P*	*r*	*P*
EQav	1	0	0.3880	0.008*
EQpd	0.3880	0.008*	1	0
PC1 of dorsal neck flexion	0	1	0.0453	0.9079
PC1 of ventral neck flexion	0.0201	0.9591	0.5065	0.1641
PC1 of lateral neck flexion	0.0011	0.9976	0.0043	0.9906
PC1 of extended neck position	0.0047	0.9891	0.0118	0.9724
PC1 of neutral neck position	0.0946	0.6676	0.0231	0.9166
PC1 of pleurodiran retracted neck	0.4683	0.6898	0.4683	0.6898
PC1 of cryptodiran retracted neck	0.0026	0.9905	0.3751	0.0778
CS of dorsal neck flexion	0	1	0.0165	0.9664
CS of ventral neck flexion	0.0366	0.9256	0.2862	0.4554
CS of lateral neck flexion	0.0006	0.9987	0.0010	0.9976
CS of extended neck position	0.0012	0.9972	0.0026	0.9940
CS of neutral neck position	0.0590	0.7893	0.0900	0.6830
CS of pleurodiran retracted neck	0.0056	0.9929	0.0056	0.9929
CS of cryptodiran retracted neck	0.0002	0.9993	0.6645	0.0007*

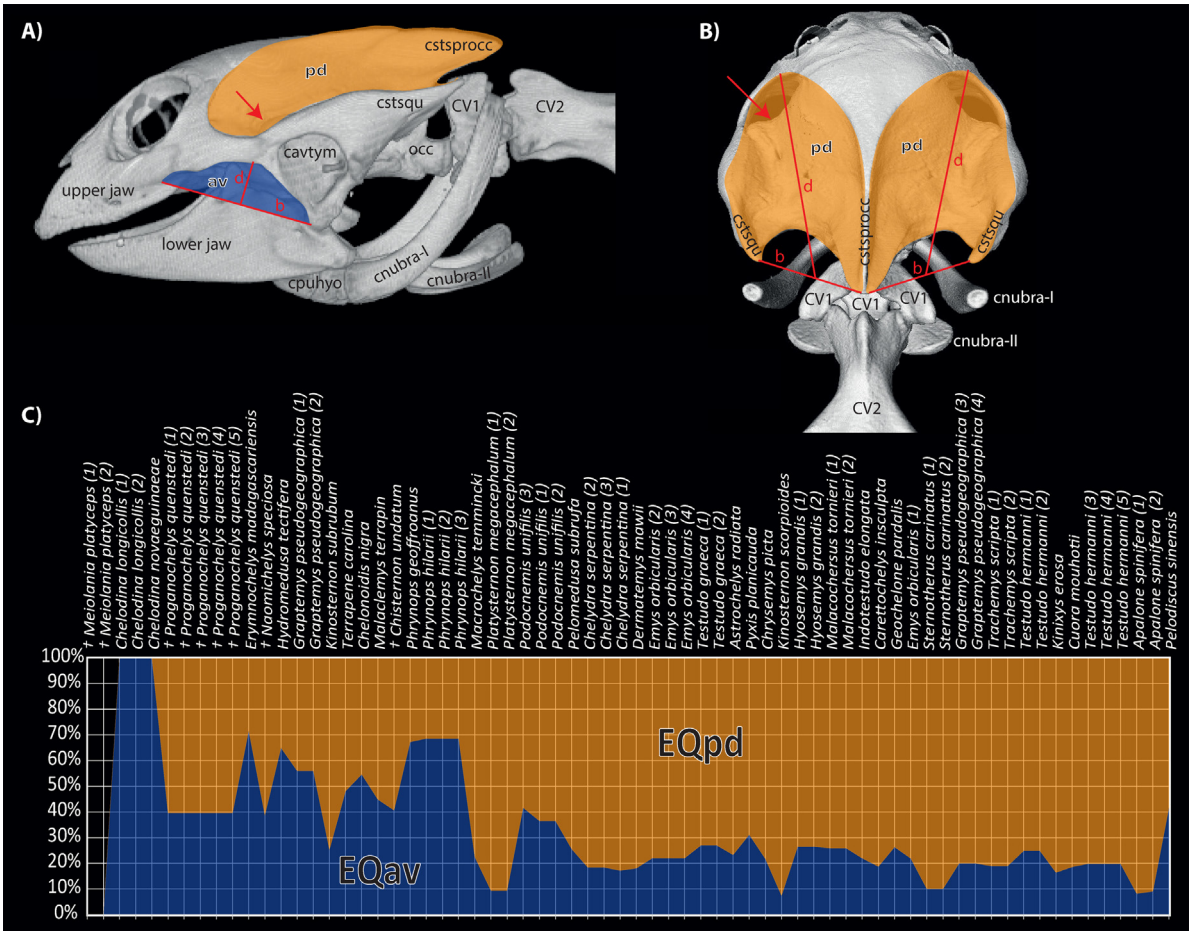

Fig. 5. (Color online.) Relative sizes of emarginations across the studied representatives of Testudinata. **A**. μCT-scanned skull of the trionychid turtle *Pelodiscus sinensis* (IW579, 100 μm resolution). Illustration of the lengths (red lines) measured for the calculation of the emargination quotient (EQ) of the anteroventral emargination (av; blue) in lateral skull view, with depth (d) divided by breadth (b). **B**. The same skull from posterodorsal view indicating the same measurements for the posterodorsal emargination (pd; orange). Note that the skull is shown in oblique view in order to visualize the position of the processus trochelaris otici (arrow; see also in A). For measurements, however, a planar dorsal skull view was used. **C**. Percentile relation of emargination quotients, ordered by increasing EQpd (for data and specimen numbers see Table 1).

Fig. 5. (Couleur en ligne.) Tailles relatives d'émargination chez les représentants de Testudinata ici étudiés. **A**. Scan-μCT de la tortue trionychide *Pelodiscus sinensis* (IW579, résolution 100 μm). Longueurs (illustrées par des lignes rouges) mesurées pour le calcul du quotient d'émargination (EQ) de l'émargination antéroventrale (av ; en bleu) en vue latérale du crâne, avec la profondeur divisée par la largeur (b). **B**. Le même crâne en vue postérodorsale indiquant les mêmes mesures pour l'émargination postérodorsale (pd ; en orangé). À noter que le crâne est présenté en vue oblique pour visualiser le processus trochelaris otici (flèche; voir aussi en **A**). Cependant, pour les mesures, une vue planaire dorsale du crâne a été utilisée. **C**. Percentile des quotients d'émargination dans l'ordre croissant de EQpd (pour la numérotation des données et des spécimens, voir Tableau 1).

specimen ID of I.W.; **SMF** = Senckenberg Forschungsinstitut und Naturmuseum Frankfurt, Frankfurt am Main, Germany; **TCT** = Teaching collection of Geowissenschaftliches Institut Universität, Tübingen, Germany.

3. Results

3.1. Neck curves

The morphospace occupied by the neck flexion in various planes (dorsal, ventral, lateral) and the neutral and extended neck curves are largely separated from the morphospace occupied by the neck retraction curves (Fig. 3).

Pleurodires have two types of lateral neck motion: a U-shaped lateral neck flexion and an S-shaped neck retraction. Both strongly differ in the morphospace that they occupy (Figs. 3 and 4). The cryptodiran and pleurodiran retraction curves are more similar to each other than equivalent neck flexions (i.e., simple bends in either of the four possible directions), but this is an artefact created by plotting the neck motion onto a two-dimensional plot, because neck retractions take place in contrary directions in these two groups of turtles (Fig. 1B–C).

The morphospace that is occupied by the curves of extended necks shows a strong overlap with that of the neutral position; however, the latter is more similar to the morphospace occupied by the curves of ventral flexion.

During dorsal and ventral flexion, the neck is limited by the carapace and plastron (cf. Fig. 2A), whereas the amount of lateral flexion is restricted by the limbs. Both

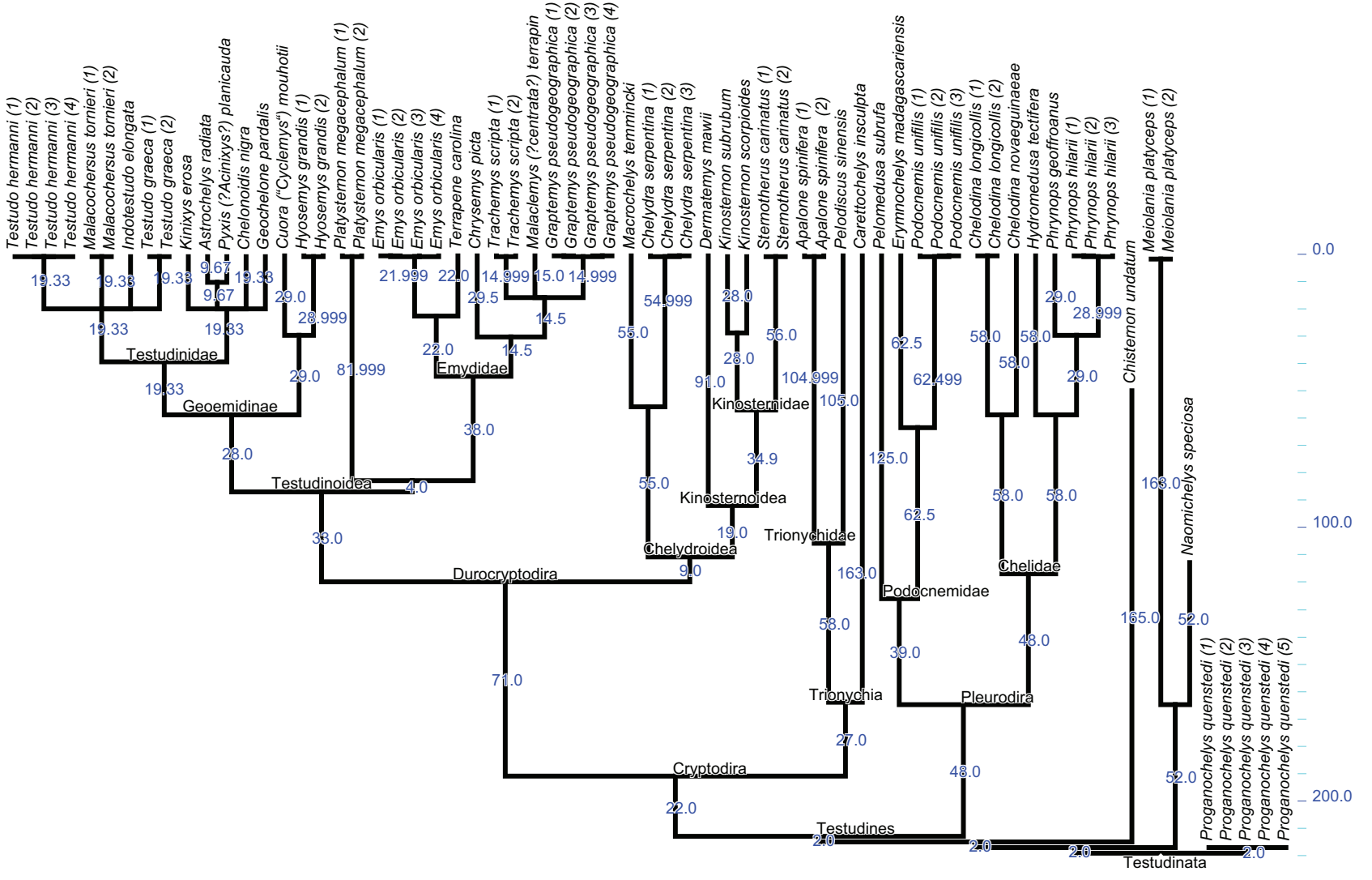

Fig. 6. (Color online.) Time scaled phylogeny of the turtle species and specimens studied herein (compare to Table 1 and Fig. 5). Numbers on the branches indicate the branch lengths in million years (my). Sections of the geological time scale equal 10 My.

Fig. 6. (Couleur en ligne.) Phylogénie à l'échelle du temps des espèces et des spécimens de tortues étudiés ici (à comparer avec le Tableau 1 et la Fig. 5). Les nombres sur les branches indiquent les longueurs des branches en millions d'années (My). Les sections de l'échelle de temps géologique représentent 10 My.

cascades are reflected in the outlines of the respective curves (Fig. S7, S9).

Curve shapes of neck flexions clearly differ between stem fossils, pleurodires, and cryptodires and all turtles are clearly separated from the outgroup species (Figs. S7–12).

3.2. Neck retraction

When plotting neck curves of lateral flexion, dorsal flexion, and all modes of retraction into one diagram, the following pattern is visible (Fig. 4). The lateral neck flexion of the outgroup (squamates) is more similar to the cryptodiran than to the pleurodiran mode of lateral flexion. Pleurodire retraction curves plot within the morphospace that is occupied by the retraction curves of cryptodires, and do not overlap with the pleurodiran lateral flexion curves.

The neck curves of cryptodires occupy a much larger morphospace than those of pleurodires (Figs. 3 and 4), which may be interpreted as an artefact of the fewer pleurodiran species studied herein (eight pleurodire vs. 26 cryptodire species). However, given the generally larger ecological diversity of cryptodires (Ernst and Barbour, 1992), the morphospace distribution may represent natural conditions.

The morphospace occupied by the neck curves of *P. quenstedti* is limited to a restricted area reflecting the ancestral low mobility of its neck (Fig. 4). The retraction curve of *P. quenstedti* (PqR in Fig. 4) plots within cryptodiran and near the pleurodiran dorsal flexion and plots nearer to the lateral flexion (PqL) than to dorsal flexion (PqD) of the same species (Fig. 4).

The minimal span tree (minimal shape difference; gray lines between points in Fig. 4) shows a close similarity between the cryptodiran retraction curves and the dorsal flexion curves.

The neck curve analyses were performed with two data sets, with seven landmarks (Fig. 2Bc–i) along the cervical column and with all ten landmarks (Fig. 2Ba–j), including the skull (exemplified in Fig. S15). Although the 7-landmark diagrams show a clearer picture, the general interpretation of the 10-landmark diagrams, with less data (no skull in most fossils), remains the same. Divergences occur due to the certain independent position and flexible orientation of the head during all neck motions (cf. Fig. 1B). The flexibility between the head and the neck is permitted mainly by the articulation between the skull and the first cervical vertebra (George and Shah, 1955a,b; Ogushi, 1913; Shah, 1963; Werneburg, 2011). Its flexibility does not influence the general distribution of neck curve shapes in morphospace.

3.3. Neck mobility and emargination

By comparing shape (PC1) and centroid size (CS) of the neck curves (Table 4) with the emargination quotients (Table 1, Fig. 5C), the following correlations were revealed (see Table 5). There is significant correlation between the centroid size of the cryptodiran retracted neck and the posterodorsal emargination ($r = 0.6645$, $P = 0.0007$). Also PC1 of the cryptodiran retracted neck ($r = 0.751$, $P = 0.0778$) and ventral neck flexion in all turtles ($r = 0.5065$, $P = 0.1641$) display a nearly statistically significant correlation with the expansion of posterodorsal emargination. For all other traits, the correlations are not statistically significant. That also includes all tested correlations between the neck parameters and the expansion of the anteroventral emargination. Significant correlation, however, exists between the expansions of both anteroventral and posterodorsal emarginations ($r = 0.388$, $P = 0.008$).

4. Discussion

The present study, firstly, uncovered distinct shape differences in the curvatures that the turtle neck shows at different positions of its motion. Secondly, only the posterodorsal emargination appears to be correlated with neck motion and the relative sizes of both anteroventral and posterodorsal marginal reductions correlate with one another.

4.1. Range of mobility and resting position

The analyses of curve shape disparity show a large range in the mobility of lateral and dorsal neck flexions and neck retractions in turtles. The ventral flexion, however, shows less disparity (Fig. 3). This corresponds to the detected differences in raw joint mobility detected by Werneburg et al. (2015a). Apparently, motion of the head to the lateral side during retraction and when searching for food to the left and right side requires more flexibility of the neck than ventral movement. The same seems to be the case for dorsal motion when snorkeling and food catching. Disparity in ventral flexion, however, appears to be less important given the flat association of the animals with the bottom soil, which is facilitated by the form of the flat plastron. Moreover, the presence of the plastron limits the range of ventral neck flexibility. This is also true for aquatic turtles, which, in theory, could largely move their neck ventrally [illustrated by Werneburg et al. (2015a)] when swimming in the water column. Particularly, in the aquatic pleurodires, the specific anatomy of the neck vertebrae, which are strongly adapted to lateral retraction (Herrel et al., 2008; Williams, 1950; Werneburg et al., 2015a,b), appears to prevent much of the ventral motion. Moreover, an excessive ventral flexion of the neck of all pleurodires and cryptodires alike would result in a strangulation of the trachea at the plastron. This appears to be the main reason for the limited ventral flexibility of the neck, because in theory, the neck allows much more ventral flexion than is performed in life (illustrated by Werneburg et al., 2015a).

One major problem of reconstructing the anatomy of the vertebral column in fossil vertebrates is the definition of the neutral, namely the resting position of the neck (Christian, 2002; Christian and Heinrich, 1998; Taylor et al., 2009). Werneburg et al. (2015a) have demonstrated that the neutral position of the turtle neck is established when the articular facets of the adjacent vertebrae fully overlap. The present study confirms that finding. The shape distribution of the extended necks, with their more or less straight orientation, occupies a different morphospace when compared to the neck curves of the neutral neck position. But it is worth mentioning that there is still much overlap between the curve lines of neutral and extended necks (Fig. 3, light and dark gray). As such, when

reconstructing a more or less straight vertebral column in a fossil model, there is a certain chance that the actual neutral position could be reconstructed. However, to accurately reconstruct the resting position, as mentioned above, the articular facets of the zygapophyses should show the greatest overlap.

4.2. Origin of cryptodiran retraction

The origin of the sideward, pleurodiran retraction mode has been illustrated to be derived from the ancestral type of neck retraction as reconstructed for *P. quenstedti* (Fig. 1C to B). To enable the retraction of the elongated pleurodiran neck, only a middle kink had to be evolved, which involved zygapophyseal elongation and other modifications of the related vertebrae, particularly in cervical five and six (Van Damme et al., 1995; Weisgram and Splechtna, 1990; Werneburg et al., 2015a, 2015b). Based on similarities of angular interrelationship along the cervical vertebral column, the vertical, cryptodiran mode of neck retraction has been hypothesized to be derived from the dorsal neck flexion found in stem turtles (Werneburg et al., 2015a). Given the non-specialized anatomy of the neck vertebrae in stem fossil taxa (Werneburg et al., 2015b) and the ability of intervertebral rotation between the cervicals that the authors detected, one could hypothesize that the cryptodiran mode of retraction could also, like the pleurodiran mode, be derived from the ancestral mode of retraction (Fig. 1C to A). In actual fact, the curve shape of the retracted neck in *P. quenstedti* is more similar to modern cryptodiran retraction than the dorsal neck flexion of *P. quenstedti* is. Namely, the dorsally flexed neck curve of *P. quenstedti* is more similar to the plesiomorphic neck mobility of the outgroup (Fig. 4). That result shows that not only the angular interrelationship, but also the overall shape of a neck curve should be taken into account to reconstruct the evolution of neck mobility.

The eighth, last cervical vertebra, which articulates with the body, enables the major angular rotation of the neck during retraction in modern turtles. Whereas cryptodires show comprehensive modifications of the eighth cervical vertebra (Dalrymple, 1979), the cervical eight of pleurodires does not show much change when compared to the ancestral condition (Williams, 1950; Werneburg et al., 2015b). Relative to the retracted neck in stem turtles (Fig. 1A; Werneburg et al., 2015a), an additional loop was acquired in pleurodires. In those, one half of the neck is laid towards one side and the other half towards the opposite side of the body. The articulation between cervical eight and the body did not have to change its anatomy because cervical eight simply swings only to the other lateral body side, hence flexibility of this articulation did not change compared to the ancestral condition. In cryptodires, a modification of the eighth cervical evolved to enable the articulation of neck and body towards a completely different, namely a vertical orientation (Herrel et al., 2008). The less specialized cervicals at the dawn of modern turtle (Testudines) evolution may have permitted a transitional, intervertebral rotation of the ancestrally retracted (laterally rotated) neck towards the vertical orientation found in cryptodires by keeping the characteristic curvature of the cervical column. The full vertical swing of the curved neck inside the body wall was then enabled by the acquisition of specialized features in the anatomy of cervical eight, namely the elongated and descending posterior zygapophyses and a shortening of the vertebral centra, in cryptodires (Werneburg et al., 2015b; Williams, 1950). Transitional taxa in this regard could be the xinjiangchelyid, sinemydid, and macrobaenid stem cryptodires, in which cervical eight is not yet as specialized as in crown cryptodires (e.g., Joyce, 2007; Parham and Hutchison, 2003; Peng and Brinkman, 1993; Zhou et al., 2014). Also, extant cryptodires show some range in the orientation of the retracted neck. It can be pure sagittal or, when enough space is available, it can be slightly rotated to the left or right body side (Werneburg et al., 2015a).

4.3. Turtle skull emargination

The temporal skull region of extant turtles shows a great morphological diversity. Besides the almost fully roofed coverage of the temporal region by dermal bones as found in extant marine turtles (similar to stem turtles), different modes of posterodorsal and anteroventral reduction occur among pleurodires and cryptodires alike (Jones et al., 2012; Kilias, 1957; Werneburg, 2012; Zdansky, 1923).

Several evolutionary, functional, and anatomical factors were postulated to have influence in shaping the temporal skull region of turtles. Ten major factors were summarized by Werneburg (2012). Among those are the reduction of bones to lower skull mass, general skull dimensions, and the specific anatomy of the ear and the related jaw musculature. Among all factors, however, neck retraction has been discussed to present the most obvious correlation to skull shape (Kilias, 1957; Zdansky, 1923). The anteroventral emargination would be associated to lateral, pleurodiran-like retraction and the posterodorsal emargination to vertical, cryptodiran-like retraction. Both emarginations would have evolved to better fit the skull into the confines of the shell during neck retraction (Kilias, 1957). Consequently, species, which lost the ability to fully withdraw the head inside the body wall (Chelonioidea, Platysternoidea), show almost no emargination and have a full bone coverage of the temporal region (Zdansky, 1923). Extinct marine turtles, such as *Toxochelys* (Hirayama, 1994; Matzke, 2009) have very large emarginations. Following the consideration of Kilias (1957), I hypothesize that, in contrast to modern marine turtles, at least some stem-chelonioids were able to fully retract their necks. The same may be true for many early, extinct lineages of Testudines, which show extended emarginations [e.g., Xinjiangchelyidae, Sinemydidae, Macrobaenidae (Zhou et al., 2014), and Baenidae].

The pleurodire taxon Pelomedusidae, as a special case, shows a strong posterodorsal emargination and only a weak anteroventral one. That resembles more a typical cryptodiran than a pleurodiran skull. As such, Kilias (1957) proposed a cryptodiran-like retraction mode for pelomedusids and hypothesized that only chelid pleurodires show pure side-neck retraction. In actual fact, however, pelomedusids clearly show a typical pleurodiran retraction and not even an intermediate between the pleurodiran

and cryptodiran mode (Weisgram and Splechtna, 1990; Werneburg et al., 2015a). Zdansky (1923) highlighted that some pelomedusids have a large anterior shell opening. As such, when the head and neck are retracted, much of the skull would still be broadly exposed to predators, resulting in a covering of the "cheek" by dermal bones for further protection. All those correlations suggest that neck retraction is most important in shaping the turtle skull and that only a few obvious additional factors need to be taken into account. However, some problems remain.

The most obvious one is that almost all pleurodires and all cryptodires show both anteroventral and posterodorsal emargination – although one emargination usually dominates in the above mentioned correlation (Fig. 5). Second, the big-headed turtles (Platysternidae) do show some degree of neck retraction but the head does not pass the border of the shell to be withdrawn inside the body wall (Werneburg et al., 2015a). Nevertheless, little posterodorsal emargination is visible in the skull of this taxon. When head and carapace contact each other dorsally in such a partly retracted neck, this small emargination may have evolved to enable an optimized use of space. As mentioned above, also extant marine turtles, presumably never fully retract their necks, and also show a little posterodorsal and even a small anteroventral emargination (Jones et al., 2012). A certain, low degree of retraction, as visible during feeding in marine turtles, may result in a similar skull shape as seen in platysternids.

The results of the present study highlight that the way how the neck is retracted in cryptodires has overwhelming influence on the shape of the posterodorsal emargination in this group. Not only the shape of the curvature alone is important. Particularly the (centroid) size of the curved neck is significantly correlated to posterodorsal skull reduction in cryptodires. Usually, the neck muscles attach via tendons to the occipital skull region or they attach via broad tendon sheets to the margin of the posterodorsal emargination (Werneburg, 2011, 2013b). Tendon sheets sparingly distribute the tensile forces acting on the skull. The broader the insertion of the tendon sheet (larger emargination) the better the force distribution.

A second important finding was that a certain correlation exists between the expansions of both types of emargination in all species observed. A reduction from one direction in the skull may require bone reduction of the opposite direction to retain the balanced integrity of the temporal skull region (but testing this assumption would require detailed biomechanic analyses). With the anteroventral reduction, the upper jaw and the postorbital bar lose their bony bridge to the ear capsule ventrally. However, in order to resist the tensile strains that arise during biting, the ligamentum quadratojugale is retained. It connects the upper jaw and the ear capsule ventrally (Jones et al., 2012; Werneburg, 2013a).

The way how both emarginations are correlated with each other and the degree of bone reduction apparently are dependent on several factors such as skull dimensions (Werneburg, 2012). Some trionychid turtles with very elongated skulls (e.g., *Apalone*, Fig. 5C), for example, show a largely expanded posterodorsal emargination but a much smaller anteroventral emargination. The extant marine turtle skulls, with their almost fully roofed coverage of the temporal region, are more rounded in their overall shape. Several chelid pleurodires have largely expanded anteroventral emarginations and extremely flat skulls, but they lack or only show little posterodorsal emargination. Some exceptions to those intuitive correlations exist. Testing parameters of skull dimensions in relation to emargination size would be worth conducting in a different study.

Based on the detected correlation, one could argue that cryptodiran retraction mode primarily influences posterodorsal and indirectly also influences anteroventral emargination. In this regard, the low degree of retraction (i.e., slightly bended neck curve, because the head hindered performance of greater flexion) found in Platysternidae (Werneburg et al., 2015a) appears to correlate with its small posterodorsal and consequently with almost no anteroventral emargination in this taxon (Table 1, Fig. 5C). The same explanation could be true for extant marine turtles, which were not studied herein but show a similar pattern of skull construction (e.g., Jones et al., 2012).

The detected correlation to cryptodiran neck retraction nicely explains the formation of the posterodorsal emargination in cryptodires; however, no strong correlation between neck retraction and temporal skull reduction was detected for pleurodiran turtles (Table 5). An obvious interpretation would be that side-necked mode of retraction does not strongly influence head anatomy. In this regard, it is worth mentioning that the neck musculature of cryptodires drastically differs from that of pleurodires; both types are highly specialized to the unique modes of retraction (George and Shah, 1955a, 1955b; Herrel et al., 2008; Hoffstetter and Gasc, 1969; Jones et al., 2012; Shah, 1963; Vallois, 1920, 1922; Werneburg, 2011). One major difference lies in the anatomy of the musculi carapacocervicocapitis (muscular units No. 81–82 of Werneburg, 2011). *M. carapacocervicocapitis lateralis Pars capitis* (No. 81) originates on the first costal plate. It inserts to the skull base, namely to the prootic and opistotic in pleurodires (Shah, 1963; Vallois, 1922) and has to be considered the major muscle for lateral retraction in pleurodires (Fig. 7D). It is completely reduced in cryptodires (except for extant marine turtles, which show only a small degree of neck retraction). The ontogenetically and phylogenetically related muscle, *M. carapacocervicocapitis medialis Pars capitis* (No. 82), is only present in cryptodires (except for trionychid turtles with their extremely flexible necks; Ogushi, 1913). It originates from a more anteromedian region of the carapace, particularly from the nuchal bone and inserts to the temporal fascia, which spans above the posterodorsal skull emargination (Fig. 7C; Werneburg, 2011, 2013a, b). It is considered to represent one of the relevant muscles for retracting the neck in the vertical plane in cryptodires (obviously in addition to *M. retrahens capiti* collique Pars carapaco-basioccipitalis, No. 88, which inserts to the skull base, and other muscular units; Werneburg, 2011).

The described muscular anatomy illustrates that neck forces of lower intensity apparently act on the occiput in pleurodires than in cryptodires and that in pleurodires the stabilization of the neck is enabled by different tensile

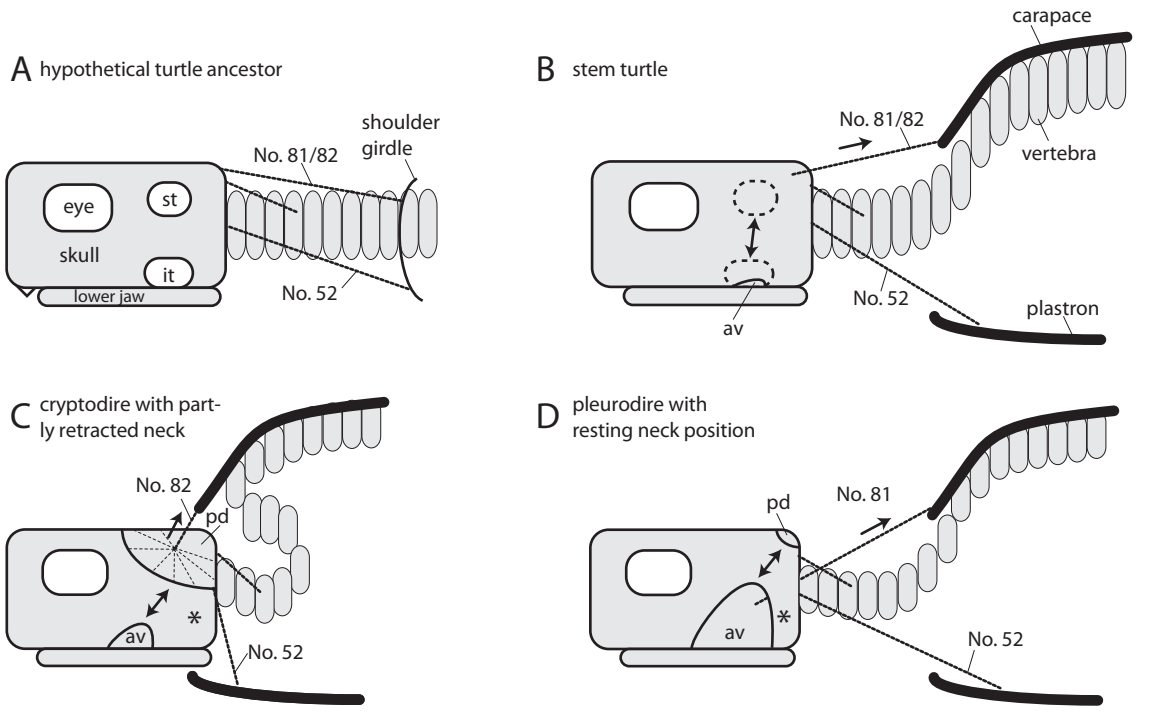

Fig. 7. Scenario for the origin of turtle anapsidy proposed in this study (provided a potential diapsid ancestor); (**A**–**B**) and explanations for the formation of skull emarginations (**B**–**D**). **A**. Hypothetical ancestor of turtles with fenestration exemplified for a diapsid. A supratemporal opening (st) is present. The infratemporal opening (if) may be present with (as fenestra) or without (as cleft) infratemporal, lower bony bar. Several neck muscles, indicated by dotted lines, insert to the skull. *M. trapezius* (herein as No. 81/82) may represent the phylogenetic mutterboden muscle for No. 81 (*M. carapacocervicocapitis lateralis Pars capitis*) and No. 82 (*M. carapacocervicocapitis medialis Pars capitis*) found in pleurodires or cryptodires, respectively (Werneburg, 2011). The muscle labelled as No. 52 represents *M. sternocleidomastoideus*, which is assumed to be homologous to *M. plastrocapitis* of turtles (Werneburg, 2011). The unlabeled dotted line indicates several further muscles originating from the neck vertebrae and inserting to the posterodorsal skull region (i.e., No. 57, 79, 80 in turtles; see text). **B**. Early stem turtle. The presence of a bony or at least a functional carapace and the correlated modification of the shoulder girdle (Lyson et al., 2013b; Nagashima et al., 2013) imply reorganization of the dorsal neck musculature (exemplified for No. 81, 82). The neck and skull have to be raised below the anterior edge of the carapace. To withstand the tensile forces, the upper and lower temporal opening close (dashed circles). A correlation between posterodorsal (occiput) and anteroventral (cheek) emargination was detected in the present study (double arrow in C–D). In this regard, one could hypothesize that the tensile forces on the posterior skull region introduce (double arrow in B) the formation of a small anteroventral emargination as found in several stem turtles (indicated by a normal line in the temporal region; av). **C**. A cryptodire with partly retracted neck. Tensile forces of dorsal neck musculature are best distributed in the skull realized by the formation of a posterodorsal emargination. Muscle No. 82 is contracted and inserts to the temporal skull region via a tendinous aponeurosis (indicated by thin dashed lines). In such way, a broad insertion to the posterodorsal skull region and hence, a better force distribution is possible. The formation of the posterodorsal emargination is correlated with the formation of the anteroventral emargination (↔). **D**. A pleurodire turtle with rested neck position. Muscle No. 81 inserts to the skull base, not to the occiput. Hence, tensile forces on the occiput are relatively low when compared to cryptodires. Only few other neck muscles insert to the occiput. **C–D**. In modern turtles, the palatoquadrate is fully fused to the braincase (indicated by *), which results in the loss of basicranial skull articulation. With the fixed quadrate, the stabilization function of the temporal bones is largely reduced, which permits their reduction in form of emarginations. A dominance of the anteroventral emargination in pleurodires is present. Some small neck muscles still need a bony insertion site at the occiput in pleurodires, whereas in cryptodires the posterodorsal emargination dominates due to the very powerful influence of muscle No. 82.

Fig. 7. Scénario pour l'origine du caractère anapsidé chez les tortues (sous réserve d'un potentiel ancêtre diapsidé) (**A**–**B**) et explications pour la formation des émarginations du cerveau (**B**–**D**). **A**. Hypothétique ancêtre des tortues avec fenestration illustrée pour un diapsidé. Une ouverture supra-temporale (st) est présente. L'ouverture infratemporale (if) peut être présente avec (fenestra) ou sans (fissure) barre inférieure osseuse infratemporale. Plusieurs muscles du cou indiqués par des lignes en pointillés s'insèrent sur le crâne. *M. trapezius* (ici N° 81/82) peut représenter, du point de vue phylogénétique, le muscle précurseur pour le N° 81 (*M. carapacocervicoapitislateralis Pars capitis*) et pour le N° 82 (*M. carapacocervicocapitis medialis Pars capitis*) trouvés chez les pleurodires et les cryptodires, respectivement (Werneburg, 2011). Le muscle marqué N° 52 représente *M. sternocleidomastoideus*, supposé être l'homologue du *M. plastrocapitis* des tortues (Werneburg, 2011). La ligne en pointillés non labélisée indique plusieurs muscles supplémentaires provenant des vertèbres du cou et s'insérant dans la région postérodorsale du crâne (c'est-à-dire N° 57, 79, 80 chez les tortues; voir le texte). **B**. Tortue de souche précoce. La présence d'une carapace osseuse ou au moins fonctionnelle et la modification induite de la gaine de l'épaule (Lyson et al., 2013b; Nagashima et al., 2013) impliquent une réorganisation de la musculature dorsale du cou (illustrée pour les N° 81, 82). Le cou et le crâne doivent être élevés sous le bord antérieur de la carapace. Pour résister aux forces de traction, les ouvertures supra- et infratemporales se ferment (cercles en tiretés). Une corrélation entre l'émargination postérodorsale (occiput) et antéroventrale (joue) a été détectée dans la présente étude (double flèche en **C**–**D**). À ce propos, une hypothèse peut être émise, selon laquelle les forces de traction sur la région postérieure du crâne introduisent (double flèche en B) la formation d'une petite émargination, telle qu'on l'observe chez différentes tortues de souche (indiquée par une ligne normale dans la région temporale ; av). **C**. Tortue cryptodire avec cou partiellement rétracté. Les forces de traction sur la musculature dorsale du cou sont mieux réparties, grâce à la formation d'une émargination postérodorsale. Le muscle N° 82 est contracté et s'insère dans la région temporale du crâne via une aponeurose tendineuse (indiquée par les fines lignes en tiretés). De cette façon, une large insertion à la région postérodorsale du crâne et, en conséquence, une meilleure répartition des forces sont possibles. La formation de l'émargination postérodorsale est corrélée à la formation de l'émargination antéroventrale (↔). **D**. Tortue pleurodire, avec le cou en position de repos. Le muscle N° 81 s'insère à la base du crâne et non à l'occiput. Ainsi, les forces de traction sur l'occiput sont relativement faibles par rapport à celles observées chez les cryptodires. Seuls quelques autres muscles du cou s'insèrent sur l'occiput. **C**–**D**. Chez les tortues actuelles,

forces, which act on the skull base rather than on the occiput.

A third, non-significant but fairly large correlation to the posterodorsal emargination was found in pleurodires and cryptodires alike, namely the curvature of the ventrally flexed neck (Table 5). When the head is flexed ventrally, the dorsal neck muscles (mm. carapacocercicocapitis lateralis/medialis Partes capitis, No. 81–82; see above) and the muscles that connect the neck with the occipital skull region (i.e., musculi collosquamosum, No. 57; cervicocapitis, No. 79; collooccipitis, No. 80; see Werneburg, 2011) are stretched, which results in a tensile force on the occiput and, as shown above, fosters the expansion of the posterodorsal emargination for better force distribution.

4.4. Evolutionary scenario for the origin of turtle anapsidy

These considerations hint to a more general view on the correlation between the unique neck and skull anatomy in turtles. The presence of the carapace in turtles and its vaulting anterior edge force the neck vertebral column to show a different orientation when compared to the dorsally convex orientation of the trunk vertebrae, which are embedded in the carapace (Fig. 7B). At resting position, either the neck has a more or less straight orientation in stem turtles or a dorsally concave orientation in crown turtles (cf. Fig. 1A; illustrated also by Werneburg et al. (2015b: Fig. S1)). Correlated with the acquisition of a shell at the dawn of turtle evolution, a reorganization of the dorsal neck musculature occurred (e.g., Gasc, 1981; Herrel et al., 2008; Lyson et al., 2013a; Werneburg, 2011). The related muscles connect the ventral face of the anterior edge of the carapace with the "sagging" neck and the skull. Different tensile forces, hence, act on the skull of turtles when compared to any possible outgroup (Fig. 7A–B). Those forces are even enlarged when the neck and head are moved during ventral neck flexion as suggested by the results of the present study. To withstand all those tensile forces – and after evolving a much longer "sagging" neck in the crown clades – the posterodorsal area of the temporal skull region must have been widened and excavated to form the posterodorsal emargination (Fig. 7B to C). This explanation could also resolve the presence of the posterodorsal emargination found in extant marine turtles, which apparently do not retract their heads inside the body.

In aquatic turtles, through the buoyancy of the water column, the gravity effect on the head and neck is eliminated. However, tensile forces on the head are still present when the turtles lay their eggs, when they bask, when hatchlings run from their nesting site to the water, and when the neck is flexed in different directions.

The tensile forces acting on the skull caused by the reorganization of the turtle trunk anatomy, i.e. the presence of a shell might be correlated to the anapsid condition of the turtle skull. Possibly, turtles plesiomorphically show an anapsid skull, which would indicate to a closer phylogenetic relationship to extinct Permian sauropsid lineages with anapsid skulls (e.g., Pareiasauria: Lee, 1997; Captorhinidae: Gaffney and Meylan, 1988; Procolophonia: Reisz and Laurin, 1991; *Eunotosaurus*: Lyson et al., 2010, 2013b). In that case, the emarginations were originally introduced into a primarily fully roofed temporal region.

In the case that turtles are diapsids, as indicated by several neontological and genetic studies (e.g., Field et al., 2014; Fong et al., 2012; Tzika et al., 2011; but see Joyce, 2015), the tensile forces acting on the skull might have forced the upper temporal fenestration to be closed in the earliest stem turtles to enable a compact skull case with more evenly distributed forces on the skull than would be possible in a diapsid skull with all its thin bony bars (Fig. 7A to B; Werneburg, 2012, 2013a) [side note: the same holds true for parareptilian lineages with fenestrations (MacDougall and Reisz, 2014; Piñeiro et al., 2012) as potential close relatives of turtles]. One of the oldest stem turtles, *P. quenstedti*, shows a fully closed temporal region. Although the tensile forces of the neck muscles might not have yet introduced excavations into the occiput (that seems to be a derived feature of crown turtles associated to elongated neck, which results in even larger tensile forces), they may have been large enough to favor the closure of the potential upper temporal opening (Fig. 7B). The closure of the upper temporal opening and subsequently of a potential infratemporal opening (as fenestrum or cleft; e.g., compare to Evans, 2008, or Piñeiro et al., 2012) – as indicated by the herein detected correlations between the cheek and the occiput skull area – could have been facilitated by extensive broadening of the squamosal, postorbital, jugal, and quadratojugal bones (sensu Müller, 2003). Following those modifications, smaller skull elements such as the supratemporal or the postfrontal may have been reduced in order to limit the number of suture lines and hence to enable the most compact temporal bone coverage.

In this context, it is worth mentioning that neck movement, including retraction, is already detectable in the embryos of turtles (Werneburg et al., 2009). Tensile forces therefore act on the developing skull from a very early ontogenic stage and the structures of potential temporal openings might be closed already during very beginning of embryonic development. The field of experimental embryology could certainly provide more insights into this question in the future.

Given the herein detected correlation between posterodorsal and anteroventral emargination in extant turtles, the tensile neck muscle forces acting on the occiput in *P. quenstedti*, which like most or even all other stem turtles was terrestrial (Joyce, 2015), might have had introduced the formation of the small anteroventral emargination found in this species (Fig. 7B). The same could be true for other stem turtles with a small anteroventral emargination including *Odontochelys semitestacea*, the sister group

le palatocarré est complètement fondu dans la boîte crânienne (indiqué par *), ce qui résulte en la perte de l'articulation basicrâniale du crâne. Avec l'os carré fixé, la fonction de stabilisation des os temporaux est largement réduite, ce qui permet leur réduction sous la forme d'émarginations. Une dominance de l'émargination antéroventrale est observée chez les pleurodires, tandis que chez les cryptodires, c'est l'émargination postérodorsale qui prédomine, en raison de l'influence très forte du muscle Nº 82.

of all other turtles (Li et al., 2008). Unlike all other known turtles, *O. semitestacea* did not have a carapace, but a plastron was developed. The condition of a half-developed shell could be ancestral for all turtles, which would mean that the plastron evolved before the carapace. However, it has been argued that *O. semitestacea* might have represented a bizarre early turtle lineage, which lost the carapace, possibly by paedomorphic truncation of carapace ossification, which frequently occurs in marine turtles (Reisz and Head, 2008, who actually suggested that *O. semitestacea* could represent the radiation of an early marine stem turtle clade), or by postmortem taphonomic processes (discussed by Rieppel, 2013, and Scheyer et al., 2013). In my opinion, specimens of *O. semitestacea* need a more comprehensive, monographic anatomical survey before drawing any final conclusions. In any case, the specific anatomy of the broadened ribs in *O. semitestacea* corresponds to certain components of a functional carapace (Lyson et al., 2014) with similar functional implications as a bony carapace (compare with the leatherback sea turtle, which secondarily evolved a functional, even more stable carapace, which, however, is anatomically not homologous to the carapace of any other turtle taxon; Delfino et al., 2013; Rieppel, 2013). As such, comparable to *P. quenstedti* and other stem Testudines, tensile neck muscle forces might have favored the closure of one or two temporal openings in *O. semitestacea*.

Given the presented scenario and the suggested tensile forces described and if recent molecular phylogenies are correct (again, see Joyce, 2015, for comprehensive discussion of the latter issue), one may expect the future discovery of a diapsid-like stem "turtle" with an *upper* temporal opening and with no carapace and no (or only slightly) broadened ribs (Fig. 7A). The anteroventral area of the temporal region in this creature may not have had incipient marginal reductions as otherwise found in stem turtles such as *O. semitestacea* and *P. quenstedti* due to the lack of carapace-related tensile neck forces transferred over the occiput to the cheek region. However, given the large morphological variation of the temporal region among amniotes (synapsids, parareptiles, and diapsids; Evans, 2008; MacDougall and Reisz, 2014), the presence of an infratemporal opening (which might anyway represent the ancestral amniote condition; Piñeiro et al., 2012), or more likely an open cleft between bones (such as in *Eunotosaurus*, squamates, and several early diapsids; Evans, 2008) was quite possibly present in the turtle ancestor. Finally, in this regard, also a fenestrated parareptile (see MacDougall and Reisz, 2014) as turtle ancestor could have lost its fenestration by the influence of changed dorsal muscle anatomy related to the acquisition of the shell in turtles.

4.5. Implications of palatoquadrate fusion to the braincase

The formation of the anteroventral emargination in turtles – besides the abovementioned correlation to the expansion of the posterodorsal emargination – remains unclear. At least neck movement appears to have little influence on shaping that skull region. In fact, tensile neck muscle forces, which appear to be correlated with the posterodorsal emargination, do not appear to influence the cheek region. During lateral neck flexion and during pleurodiran retraction, tensile forces certainly strongly act on the skull. However, the related muscles ventrally insert on the braincase (see above; No. 81) or insert on the ear capsule (*M. plastrocapitis*; Werneburg, 2011: No. 52), but not on the cheek (Fig. 7D). Certainly, some forces also act on the anteroventral area of the temporal region during sideward movements via the stretched skin (in only one turtle species a lateral muscle is known to attach to the "cheek" laterally; Werneburg, 2011: No. 44). Those transmitted forces, however, may not have such an impact on marginal reduction because they come from caudal direction whereas marginal excavation opens ventrally.

During turtle evolution, the palatoquadrate became strongly fixed to the braincase (Fig. 7B–C), resulting in the immobility of the basicranial articulation (Eßwein, 1992; Rabi et al., 2013; Sterli and De La Fuente, 2010). One possible explanation for that pattern is that this permitted the cranium as a whole to withstand higher biting forces that might have been related to the potential herbivorous behavior in stem turtles (King, 1996; Werneburg, 2014). For that, a mobile quadrate, as present in squamates (e.g., Iordansky, 1990), would be disadvantageous. Another, not necessarily incompatible explanation is that the palatoquadrate was fixed in order to withstand the tensile forces during neck retraction, particularly in the crown turtles with their longer neck (and stronger tensile forces) and in pleurodires in particular with their side-necked retraction mode. With the fusion of the palatoquadrate to the braincase, the temporal skull roof lost its function of stabilization of the quadrate. Consequently, bones of the temporal region could be reduced. Whereas the more posterodorsal bones may still be required as muscle attachment sites and to withstand and to buffer tensile neck forces, the anteroventral area of the temporal region may have been selected for greater flexibility, which would have favored bone reduction. In pleurodires, in which posterodorsal tensile forces are smaller than in cryptodires due to the lack of temporal skull insertion of dorsal neck muscles (Fig. 7D), the extent of this flexibility may be more pronounced in order to better fit the skull within the confines of the shell during lateral retraction (sensu Kilias, 1957). With a reduction of dorsal neck muscles in pleurodires, the anteroventral emargination can expand up to the posterodorsal part of the temporal region, whose bones finally can be fully reduced as seen in some chelids such as *Chelus fimbricatus*.

It has been argued that internal forces created by the jaw musculature may have a certain impact on the architecture of the temporal region (reviewed by Werneburg, 2012). Initial cladistic (Jones et al., 2012; Werneburg, 2013b) and initial embryonic studies of the jaw musculature (Rieppel, 1990; Tvarožková, 2006), however, did not reveal a tight correlation between jaw muscles and temporal bone arrangement. But this field apparently requires more observation.

With the fusion of the palatoquadrate to the braincase in extant turtles, which may have been initiated by the tensile neck forces (see above), the jaw musculature (i.e., m. adductor mandibulae externus; Werneburg, 2011; Nos. 17–21) is forced to bend around the ear capsule. Pleurodires

bend the musculature around the processus trochlearis pterygoidei, which is more anterior than the quadrate fixation. In such way, the muscle part, which bends around that processus, can be found in a more anteriorly region of the muscle. Cryptodires, however, bend their jaw musculature around a processus trochlearis otici (Fig. 5A–B), which is formed more posteriorly by the quadrate and the prootic (Werneburg, 2013b). In both types, a part of the jaw musculature is in front and a part is behind the muscle bend. To permit maximal muscle fiber length and hence muscle force, pleurodires and cryptodires show caudally elongated supraoccipital and squamosal crests as enlarged jaw muscle origin sites. Already stem cryptodires had such crista associated to an incipiently developed processus trochlearis otici (Rabi et al., 2014). Those crests certainly increased the size of the posterodorsal emargination in various taxa. They provide a larger area for tendinous neck muscle attachments and hence, promoted as a kind of back coupling, an even more effective cryptodiran-like retraction (e.g., in trionychids). In pleurodires, a part of the external jaw musculature originates posteriorly at the ear capsule, which is an alternative or additional way of fiber elongation (Werneburg, 2013b).

The arguments presented here that explain the shaping of the temporal skull region in turtles are certainly limited due to the exclusive focus of the present study on neck curvatures. To which degree other cranial and postcranial factors contribute cannot be determined herein. It has been argued by Lyson and Joyce (2009) that some extinct baenid turtles may have evolved a full coverage of their temporal skull region in response to the predatory pressure caused by mammals after the K/Pg boundary. I will not discard this hypothesis because turtle skull shape diversity appears to correspond to several other environmental and anatomical factors than the mode of neck motion or the stabilization of the palatoquadrate alone (Werneburg, 2012).

5. Conclusions

The similarity in the shape of the retracted necks in cryptodires and stem turtles provides new evidence that neck retraction evolved only once within turtle evolution. The ancestrally retracted neck was modified by a horizontal S-bend in pleurodires (Werneburg et al., 2015a) and by an intervertebral rotation towards the vertically oriented neck in cryptodires.

The use of geometric morphometric methods uncovers a tight correlation between neck retraction and ventral neck flexion with the occiput skull reduction in turtles. The extent of cheek reduction, which is mainly considered as a consequence of palatoquadrate fixation and a related loss of function of the temporal bone coverage, is somehow correlated to the extent of the posterodorsal emargination. Despite the presented, obvious correlations that explain much of the turtle skull diversity, many other factors have to be taken into account to fully understand the formation of the temporal skull region in turtles, including specific environmental and anatomical pressures. In future studies finite element analyses should test the presented interpretations of the influence of neck motion to the shape of the temporal skull region in turtles.

The great mobility of the turtle neck is unique among vertebrates and its origin has to be associated to the evolution of the turtle shell (Werneburg et al., 2015a). Finally, in a functional chain – shell → neck → head – the neck motion strongly influences skull shape by closing possible previous fenestration(s) in a potential diapsid ancestor and by influencing marginal reduction of the temporal skull region of turtles.

Acknowledgements

Márton Rabi, Michel Laurin, Juliana Sterli, and one anonymous reviewer provided very valuable suggestions to improve the manuscript. I am also grateful to Juliane K. Hinz, Walter G. Joyce, Daisuke B. Koyabu, Marcelo R. Sánchez-Villagra, Torsten M. Scheyer, Rainer R. Schoch, and Adrian Tröscher for discussion and support. I thank Michel Laurin and Nathalie Bardet for the invitation to write this paper. The study was supported by Advanced Postdoc Mobility Fund P300P3_158526 of SNF and by DFG fund WE 5440/1-1 granted to I.W., by a DFG fund JO 928/1-1 granted to W.G.J., and by SNF fund 31003A_149605 granted to M.R.S.-V.

Appendix A. Supplementary data

Supplementary data associated with this article can be found, in the online version, at doi:10.1016/j.crpv.2015.01.007.

References

Bramble, D.M., Hutchinson, J.H., Legler, J.M., 1984. Kinosternid shell kinesis: structure, function and evolution. Copeia 1984 (2), 456–475.
Callister, R.J., Pierce, P.A., McDonagh, J.C., Stuart, D.G., 2005. Slow-tonic muscle fibers and their potential innervation in the turtle, *Pseudemys (Trachemys) scripta elegans*. J. Morphol. 264 (1), 62–74.
Christian, A., 2002. Neck posture and overall body design in sauropods. Mitteilungen des Museums für Naturkunde Berlin. Geowissenschaftliche Reihe 5, 271–281.
Christian, A., Heinrich, W.-D., 1998. The neck posture of *Brachiosaurus brancai*. Mitteilungen des Museums für Naturkunde Berlin,. Geowissenschaftliche Reihe 1, 73–80.
Dalrymple, G.H., (PhD) 1975. Variation in the cranial feeding mechanism of turtles of the genus *Trionyx* GEOFFROY. University of Toronto.
Dalrymple, G.H., 1979. Packaging problems of head retraction in trionychid turtles. Copeia 4, 655–660.
Delfino, M., Scheyer, T.M., Chesi, F., Fletcher, T., Gemel, R., MacDonald, S., Rabi, M., Salisbury, S.W., 2013. Gross morphology and microstructure of type locality ossicles of *Psephophorus polygonus* Meyer 1847 (Testudines, Dermiochelyidae). Geol. Mag. 150, 767–782.
Ernst, C.H., Barbour, R.W., 1992. Turtles of the World. Smithsonian Institution Scholarly Press, Washington.
Eßwein, S.E., 1992. Zur phylogenetischen und ontogenetischen Entwicklung des akinetischen Craniums der Schildkröten. Natürliche Konstruktionen – Mitteilungen des SFB 230 (7), 51–55.
Evans, S.E., 2008. The Skull of Lizards and Tuatara. In: Gans, C., Gaunt, A.S., Adler, K. (Eds.), Morphology H. The Skull of the Lepidosauria, vol. 20. Society for the Study of Amphibians and Reptiles, Salt Lake City, pp. 1–347.
Felsenstein, J., 1985. Phylogenies and the comparative method. Am. Nat. 125, 1–15.
Field, D.J.A., Gauthier, J., King, B.L., Pisani, D., Lyson, T.R., Peterson, K.J., 2014. Toward consilience in reptile phylogeny: miRNAs support an archosaur, not lepidosaur, affinity for turtles. Evol. Dev. 16 (4), 189–196.
Fong, J.J., Brown, J.M., Fujita, M.K., Boussau, B., 2012. A phylogenomic approach to vertebrate phylogeny supports a turtle-archosaur affinity and a possible paraphyletic Lissamphibia. Plos One 7 (11), e48990.

Gaffney, E.S., 1979. Comparative cranial morphology of recent and fossil turtles. Bull. Am. Mus. Nat. Hist. 164 (2), 67–376.
Gaffney, E.S., 1983. The cranial morphology of the extinct horned turtle, *Meiolania platyceps*, from the Pleistocene of Lord Howe Island, Australia. Bull. Am. Mus. Nat. Hist. 175 (art. 4), 361–480.
Gaffney, E.S., 1985. The cervical and caudal vertebrae of the cryptodiran turtle, *Meiolania platyceps*, from the Pleistocene of Lord Howe Island, Australia. Am. Mus. Novitates 2805, 1–29.
Gaffney, E.S., 1990. The comparative osteology of the Triassic turtle *Proganochelys*. Bull. Am. Mus. Nat. Hist. 194, 1–263.
Gaffney, E.S., Meylan, P.A., 1988. A Phylogeny of Turtles. In: Benton, M.J. (Ed.), The Phylogeny and Classification of the Tetrapods Volume 1: Amphibians, Reptiles, Birds, Special Vol. 35A. Clarendon Press, Oxford, pp. 157–219.
Gasc, 1981. Axial musculature. In: Gans, C., Parson, T.S. (Eds.), Biology of the Reptilia, vol. II. Academic Press, London, pp. 355–435.
George, J.C., Shah, R.V., 1955a. The myology of the head and neck of the Indian tortoise, *Testudo elegans*. J. Anim. Morphol. Physiol. 2 (1), 1–13.
George, J.C., Shah, R.V., 1955b. The myology of the head and the neck of the common indian pond turtle, *Lissemys punctata granosa* SCHOEPFF. J. Anim. Morphol. Physiol. 1 (1), 1–12.
Hammer, O., Harper, D.A.T., Ryan, P.D., 2001. PAST: palaeontological statistics software package for education and data analysis. Palaeontol. Elect. 4 (1, art. 4) http://palaeo-electronica.org/2001_1/past/issue1_01.htm
Herrel, A., Van Damme, J., Aerts, P., 2008. Cervical Anatomy and Function in Turtles. In: Wyneken, J., Godfrey, M.H., Bels, V. (Eds.), Biology of Turtles. CRC Press, Boca Raton, London, New York, pp. 163–185.
Hirayama, R., 1994. Phylogenetic systematics of chelonioid sea turtles. The Island Arc 3, 270–284.
Hoffstetter, R., Gasc, J.P., 1969. Vertebrae and Ribs of Modern Reptiles. In: Gans, A.C., Bellairs, d'A., Parsons, A.T. (Eds.), Biology of the Reptilia, 1. Academic Press, London.
Iordansky, N.N., 1990. Evolution of cranial kinesis in lower tetrapods. Netherlands J. Zoology 40 (1–2), 32–54.
Jamniczky, J.A., Russell, A.P., 2007. *Chrysemys picta* (On-line). Digital Morphology, Accessed September 16, 2014 at http://digimorph.org/specimens/Chrysemys_picta/
Jones, M.E.H., Werneburg, I., Curtis, N., Penrose, R., O'Higgins, P., Fagan, M.J., Evans, S.E., 2012. The head and neck anatomy of sea turtles (Cryptodira: Chelonioidea) and skull shape in Testudines. Plos One 7 (11), e47852, http://dx.doi.org/10.1371/journal.pone.0047852
Joyce, W.G., 2007. Phylogenetic relationships of Mesozoic turtles. Bull. Peabody Mus. Nat. Hist. 48 (1), 3–102.
Joyce, W.G., 2015. The origin of turtles: a paleontological perspective. J. Exp. Zool., B, Mol. Dev. Evol. (in press).
Joyce, W.G., Parham, J.F., Lyson, T.R., Warnock, R.C.M., Donoghue, P.C.J., 2013. A divergence dating analysis of turtles using fossil calibrations: an example of best practice. J. Paleontol. 87 (4), p612–p634.
Kilias, R., 1957. Die funktionell-anatomische und systematische Bedeutung der Schläfenreduktion bei Schildkröten. Mitteilungen aus dem Zoologischen Museum in Berlin 33 (2), 307–354.
King, G., 1996. Reptiles and Herbivory. Chapman & Hall, London.
Landberg, T., Mailhot, J.D., Brainerd, E.L., 2003. Lung ventilation during treadmill locomotion in a terrestrial turtle, *Terrapene carolina*. J. Exp. Biol. 206, 3391–3404.
Lee, M.S.Y., 1997. Pareiasaur phylogeny and the origin of turtles. Zool. J. Linnean Soc. 120, 197–280.
Legler, J.M., 1960. Natural History of the Ornate Box Turtle, *Terrapene ornata ornata* Agassiz. University of Kansas Publications. Mus. Nat. Hist. 11, 527–669.
Li, C., Wu, X.C., Rieppel, O., Wang, L.T., Zhao, L.J., 2008. An ancestral turtle from the Late Triassic of southwestern China. Nature 456, 497–501.
Lyson, T.R., Joyce, W.G., 2009. A new species of *Palatobaena* (Testudines: Baenidae) and a maximum parsimony and Bayesian phylogenetic analysis of Baenidae. J. Paleontol. 83 (3), 457–470.
Lyson, T.R., Bever, G.S., Bhullar, B.-A.S., Joyce, W.G., Gauthier, J.A., 2010. Transitional fossils and the origin of turtles. Biol. Lett. 6, 830–833.
Lyson, T.R., Bever, G.S., Scheyer, T.M., Hsiang, A.Y., Gauthier, J.A., 2013a. Evolutionary origin of the turtle shell. Curr. Biol. 23, 1–7.
Lyson, T.R., Bhullar, B.-A.S., Bever, G.S., Joyce, W.G., de Queiroz, K., Abzhanov, A., Gauthier, J.A., 2013b. Homology of the enigmatic nuchal bone reveals novel reorganization of the shoulder girdle in the evolution of the turtle shell. Evol. Dev. 15 (5), 317–325.
Lyson, T.R., Schachner, E.R., Botha-Brink, J., Scheyer, T.M., Lambertz, M., Bever, G.S., Rubidge, B.S., de Queiroz, K., 2014. Origin of the unique ventilatory apparatus of turtles. Nat. Commun. 5 (5211), 1–11.
MacDougall, M.J., Reisz, R.R., 2014. The first record of nyctiphruretid parareptile from the Early Permian of North America, with a discussion of parareptilian temporal fenestration. Zool. J. Linnean Soc. 172 (3), 616–630.
Maddison, W.P., Maddison, D.R., 2011. Mesquite: a modular system for evolutionary analysis. Version 2. 75. http://mesquiteproject.org
Matzke, A.T., 2009. Osteology of the skull of *Toxochelys* (Testudines, Cheloniodea). Palaeontograph. Abteilung A 288 (4), 93–150.
Müller, J., 2003. Early loss and multiple return of the lower temporal arcade in diapsid reptiles. Naturwissenschaften 90, 473–476.
Nagashima, H., Hirasawa, T., Sugahara, F., Takechi, M., Usuda, R., Sato, N., Kuratani, S., 2013. Origin of the unique morphology of the shoulder girdle in turtles. J. Anat. 223, 547–556.
Ogushi, K., 1913. Anatomische Studien an der japanischen dreikralligen Lippenschildkröte (*Trionyx japanicus*), II. Mitteilung: Muskel- und peripheres Nervensystem. Morphologisches Jahrbuch 46 (3+4), 299–562.
Parham, J.F., Hutchison, J.H., 2003. A new eucryptodiran turtle from the Late Cretaceous of North America (Dinosaur Provincial Park, Alberta, Canada). J. Vertebr. Paleontol. 23, 783–798.
Peng, J.-H., Brinkman, D.B., 1993. New material of *Xinjiangchelys* (Reptilia: Testudines) from the Late Jurassic Qigu Formation (Shishugou Group) of the Pingfengshan locality, Junggar Basin, Xinjiang. Can. J. Earth Sci. 30, 2013–2026.
Piñeiro, G., Ferigolob, J., Ramosa, A., Laurin, M., 2012. Cranial morphology of the Early Permian mesosaurid *Mesosaurus tenuidens* and the evolution of the lower temporal fenestration reassessed. C. R. Palevol 11, 379–391.
Rabi, M., Zhou, C.-F., Wings, O., Ge, S., Joyce, W.G., 2013. A new xinjiangchelyid turtle from the Middle Jurassic of Xinjiang, China and the evolution of the basipterygoid process in Mesozoic turtles. BMC Evol. Biol. 13 (203), 1–28.
Rabi, M., Sukanov, V.B., Egorova, V.N., Danilov, I., Joyce, W.G., 2014. Osteology, relationships, and ecology of *Annemys* (Testudines, Eucryptodira) from the Late Jurassic of Shar Teg, Mongolia and phylogenetic definitions for Xinjiangchelyidae, Sinemydidae, and Macrobaenidae. J. Vertebr. Paleontol. 34 (2).
Reisz, R.R., Laurin, M., 1991. *Owenetta* and the origin of turtles. Nature 349, 324–326.
Reisz, R.R., Head, J.J., 2008. Turtle origins out to sea. Nature 456, 450–451.
Rieppel, O., 1990. The structure and development of the jaw adductor musculature in the turtle *Chelydra serpentina*. Zool. J. Linnean Soc. 98, 27–62.
Rieppel, O., 2013. The Evolution of the Turtle Shell. In: Gardner, J., Brinkman, D., Holroyd, P. (Eds.), Vertebrate Paleobiology and Paleoanthropology Series, Morphology and Evolution of Turtles. Springer, Dordrecht, Heidelberg, New York, London, pp. 51–61.
Rohlf, F.J., Slice, D.E., 1990. Extensions of the Procrustes method for the optimal superimposition of landmarks. Syst. Zool. 39, 40–59.
Scanlon, T.C., 1982. Anatomy of the neck of the western painted turtle (*Chrysemys picta belli* Gray; Reptilia, Testudinata) from the perspective of possible movements in the region. The University of Michigan, Michigan.
Scheyer, T.M., Werneburg, I., Mitgutsch, C., Delfino, M., Sánchez-Villagra, M.R., 2013. Three ways to tackle the turtle: integrating fossils, comparative embryology and microanatomy. In: Gardner, J., Brinkman, D., Holroyd, P. (Eds.), Vertebrate Paleobiology and Paleoanthropology Series. Springer, Dordrecht, Heidelberg, New York, London, pp. 63–70.
Shah, R.V., 1963. The neck musculature of a cryptodire (*Deirochelys*) and a pleurodire (*Chelonida*) compared. Bull. Mus. Comp. Zool. 129 (6), 343–368.
Sterli, J., De La Fuente, M.S., 2010. Anatomy of *Condorchelys antiqua* Sterli, 2008, and the origin of the modern jaw closure mechanism in turtles. J. Vertebr. Paleontol. 30 (2), 351–366.
Taylor, M.P., Wedel, M.J., Naish, D., 2009. Head and neck posture in sauropod dinosaurs inferred from extant animals. Acta Palaeontol. Pol. 54 (2), 213–220.
Thomson, R.C., Shaffer, H.B., 2010. Sparse supermatrices for phylogenetic inference: taxonomy, alignment, rogue taxa, and the phylogeny of living turtles. Syst. Biol. 59 (1), 42–58.
Tvarožková, B., (Masters thesis) 2006. Development of the Temporal Emargination in Turtles and the Temporal Fenestration in Crocodilians: The origin of an Anapsid-Like Chelonian Skul. Charles University, Prague.
Tzika, A.C., Helaers, R., Schramm, G., Milinkovitch, M.C., 2011. Reptilian-transcriptome v1.0, a glimpse in the brain transcriptome of five divergent Sauropsida lineages and the phylogenetic position of turtles. EvoDevo 2 (19), 1–17.
Van Damme, J., Aerts, P., 1997. Kinematics and functional morphology of aquatic feeding in Australian snake-necked turtles (Pleurodira; Chelodina). J. Morphol. 233, 113–125.

Van Damme, J., Aerts, P., De Vree, F., 1995. Kinematics of the escape head retraction in the common snake-necked turtle, *Chelodina longicollis* (Testudines: Pleurodira: Chelidae). Belg. J. Zool. 125, 215–235.

Vallois, H.V., 1920. Les muscles de l'épisome chez les Chéloniens. Bull. Soc. Sci. Med. Biol. Montpellier II (I), 76–78.

Vallois, M.H.V., 1922. Les transformations de la musculature de l'episome chéz les vertébrés. Arch. Morphol. Gen. Exp. 13, 1–538.

Weisgram, J., Splechtna, H., 1990. Intervertebral movability in the neck of two turtle species (*Testudo hermanni hermanni*, *Pelomedusa subrufa*). Zoologische Jahrbücher. Abteilung für Anatomie und Ontogenie der Tiere 120, 425–431.

Werneburg, I., 2011. The cranial musculature in turtles. Palaeontol. Electron. 14 (2), 15a, 99 pages.

Werneburg, I., 2012. Temporal bone arrangements in turtles: an overview. J. Exp. Zool., B, Mol. Dev. Evol. 318, 235–249.

Werneburg, I., 2013a. The tendinous framework in the temporal skull region of turtles and considerations about its morphological implications in amniotes: a review. Zool Sci. 31 (3), 141–153.

Werneburg, I., 2013b. Jaw musculature during the dawn of turtle evolution. Org. Divers. Evol. 13, 225–254.

Werneburg, I., 2014. Konvergente Evolution herbivorer Landwirbeltiere. In: Maier, W., Werneburg, I. (Eds.), Schlüsselereignisse der organismischen Makroevolution. Scidinge Hall Verlag, Zürich, pp. 295–331.

Werneburg, I., Hugi, J., Müller, J., Sánchez-Villagra, M.R., 2009. Embryogenesis and ossification of *Emydura subglobosa* (Testudines, Pleurodira, Chelidae) and patterns of turtle development. Dev. Dyn. 238 (11), 2770–2786, http://dx.doi.org/10.1002/dvdy.22104

Werneburg, I., Hinz, J.K., Gumpenberger, M., Volpato, V., Natchev, N., Joyce, W.G.A., 2015a. Modeling neck mobility in fossil turtles. J. Exp. Zool., B, Mol. Dev. Evol. (in press).

Werneburg, I., Wilson, L.A.B., Parr, W.C.H., Joyce, W.G., 2015b. Evolution of neck vertebral shape and neck retraction at the transition to modern turtles: an integrated geometric morphometric approach. Syst. Biol. 64 (2), 187–204.

Williams, E.E., 1950. Variation and selection in the cervical central articulations of living turtles. Bull. Am. Mus. Nat. Hist. 94 (9), 509–561.

Zdansky, O., 1923. Über die Temporalregion des Schildkrötenschädels. Bull. Geol. Instit. Univ. Upsala 19, 89–114.

Zhou, C.-F., Rabi, M., Joyce, W.G., 2014. A new specimen of *Manchurochelys manchoukuoensis* from the Early Cretaceous Jehol Biota of Chifeng, Inner Mongolia, China and the phylogeny of Cretaceous basal eucryptodiran turtles. BMC Evol. Biol. 14 (77), 1–16.